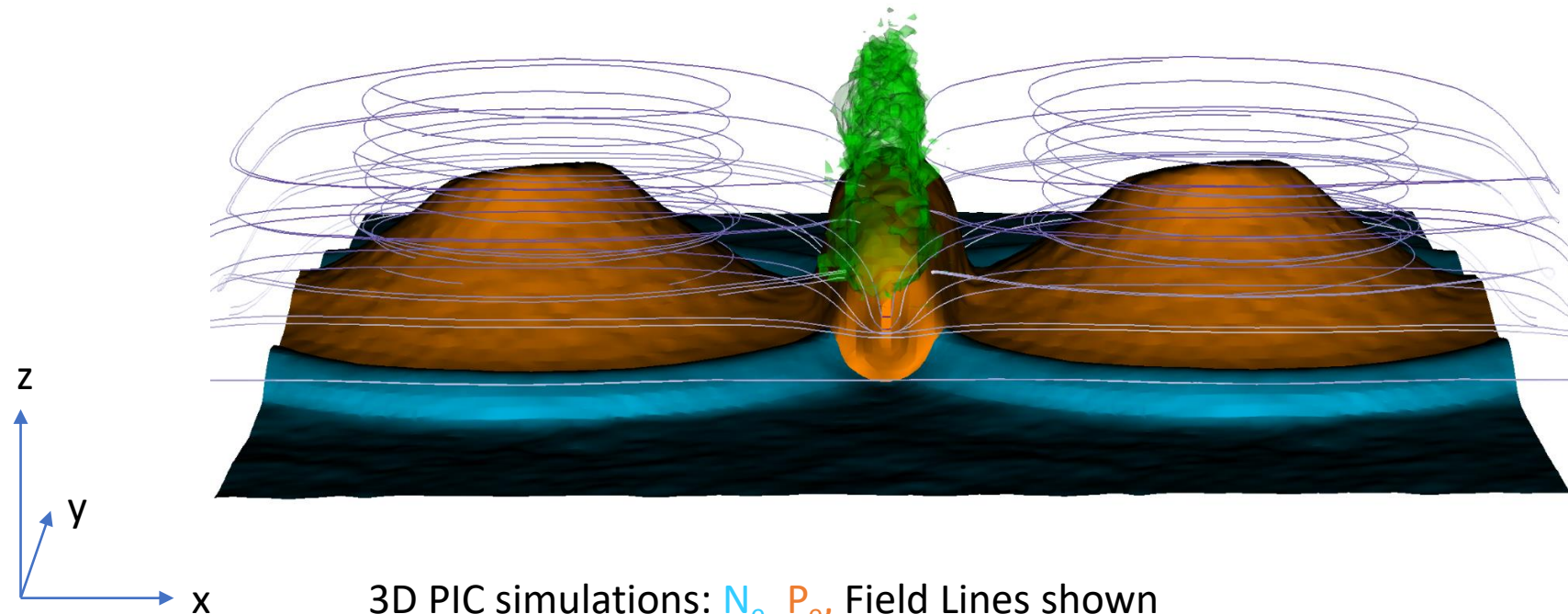
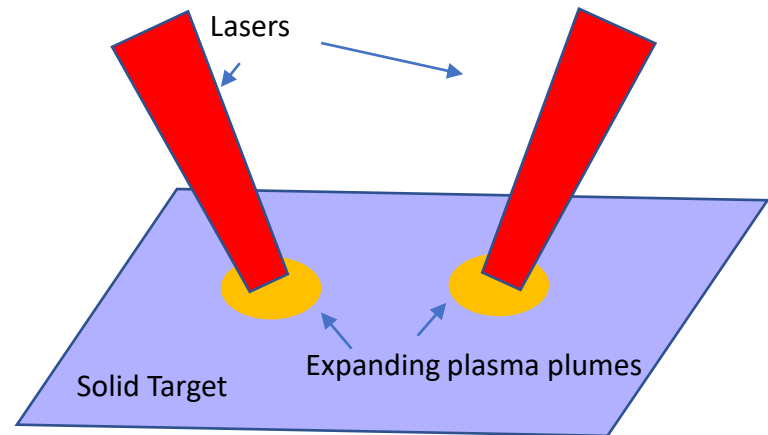


3-D magnetic reconnection in laser-driven plasmas: Novel modeling provides insight into laboratory and astrophysical current sheets



Jack Matteucci, Princeton University

Advisors: Will Fox, Amitava Bhattacharjee

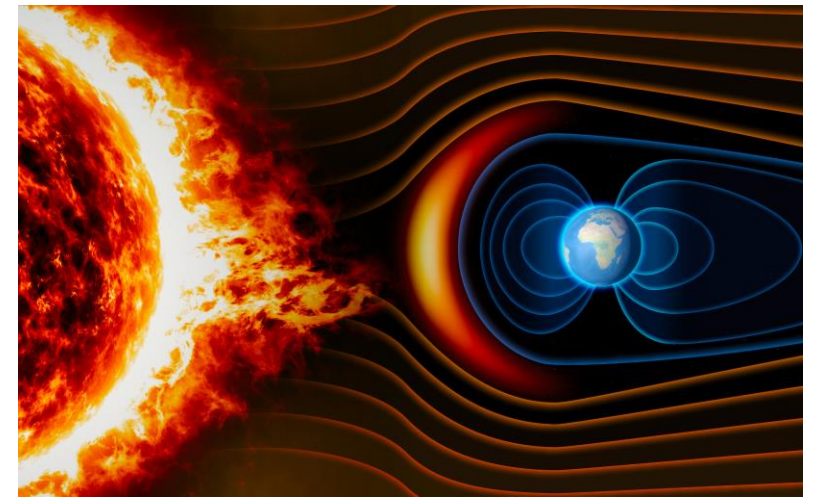
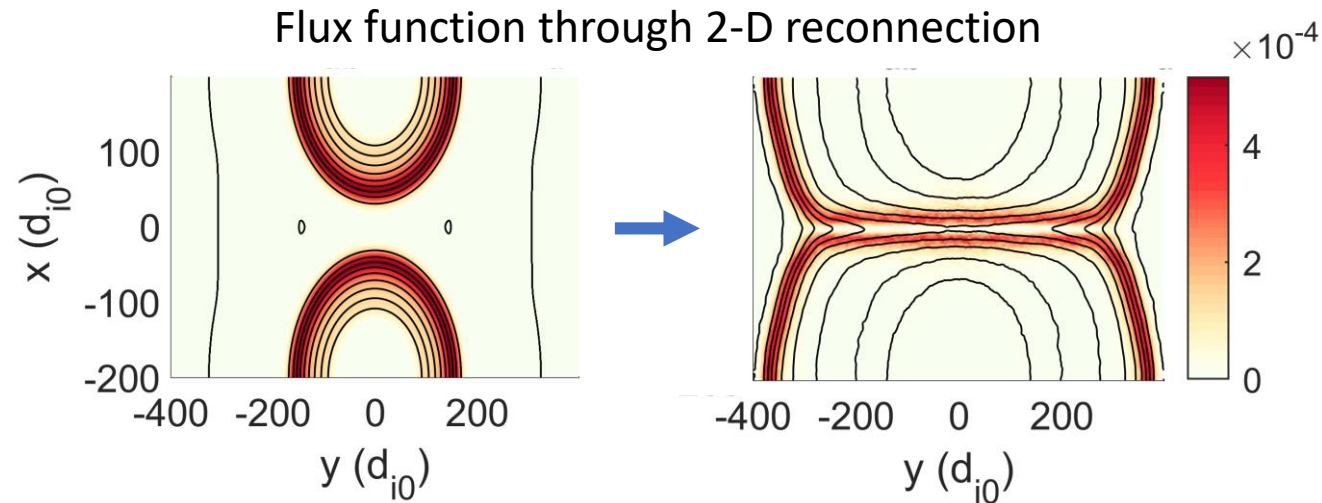
Collaborators: Derek Schaeffer, Kirill Lezhnin

Presentation Outline

- Laser-produced high-energy density plasmas can study astrophysical-like reconnection in the laboratory.
- First full 3-D kinetic simulations modeling self-consistent evolution of HED reconnection experiments
 - Field generation mechanisms during plasma ablation process
 - Reconnection current sheet evolution
- **Biermann Battery mediated reconnection**
 - Novel 3-D reconnection mechanism that could be relevant in space plasmas
- Significant other 3-D modifications to HED reconnection experiments
- Ion Weibel instability drives generation of 50 T magnetic fields in large ablation experiments

Magnetic Reconnection is ubiquitous throughout plasmas physics

- Magnetic reconnection is the process by which magnetic fields, threaded through plasma, undergo a fundamental change in topology
- Rapid exchanges of magnetic field energy into the plasma
- This process is important for:
 - Solar flares
 - the sawtooth instability in toroidal devices,
 - interactions between the solar wind and magnetosphere,
 - in the helio-sheath,
 - in magnetized astrophysical shocks
- Likely responsible for particle acceleration
- Typically studied from a 2-D perspective



Earth.com

Laser Driven Experiments provide valuable insights into reconnection

Why High Energy Density Reconnection?

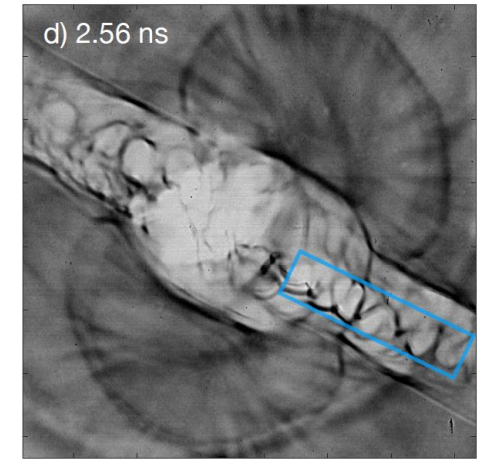
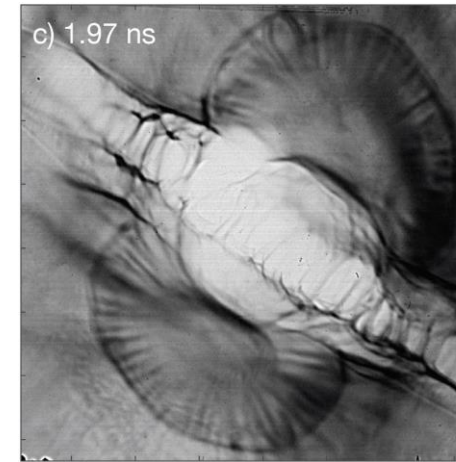
Laboratory experiments are:

- Reproducible
- Show the whole reconnection evolution, from the global scale down to kinetic scale.

HED experiments are getting close to normalized astrophysical scales ($L \gg d_i$)

- Nilson et. al. (PRL 2006 at Vulcan Facility) observed evidence of faster than Sweet-Parker reconnection.
- Particle acceleration predicted (Fox PoP 2017, Tororica PRL 2016)
- Recent results on Omega EP observed a turbulent sea of plasmoids.

Recent Omega EP Experiments performed by W. Fox, et al.



Shown below, HED reconnection experiments are able to probe closer to astrophysical scales ($S \gg 1000$) than every before!

Parameter	MRX	Vulcan	SG-II	Omega EP	NIF
System Size (L/d_i)	5-10	12-25	40-80	50-100	200
Lundquist Number $S = L V_A / \eta$	250	500	1000	1500	1500-10 ⁴

HED Experiments use Biermann Battery Field Generation for large (100 T) fields

- Possible source of seed field, subsequently amplified to cosmic magnetic fields
- Operates when gradients of the n_e and T_e are not collinear
- Magnetic fields of order MG in HED plasmas.

Generalized Ohm's law:

$$\mathbf{E} = -\mathbf{v} \times \mathbf{B} + \frac{\mathbf{j} \times \mathbf{B}}{n_e e} - \frac{\nabla p_e}{n_e e} - \frac{\nabla \cdot \Pi_e}{n_e e} + \frac{\mathbf{R}_{ei}}{n_e e},$$

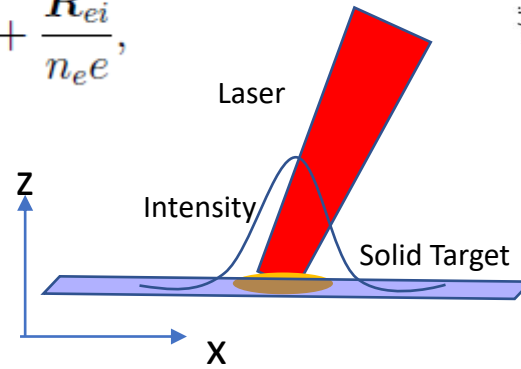
$$\partial_t \mathbf{B} = -\nabla \times \mathbf{E}$$

Biermann Battery term:

$$\frac{\partial \mathbf{B}}{\partial t} = \nabla \times \frac{1}{n_e e} \nabla p$$

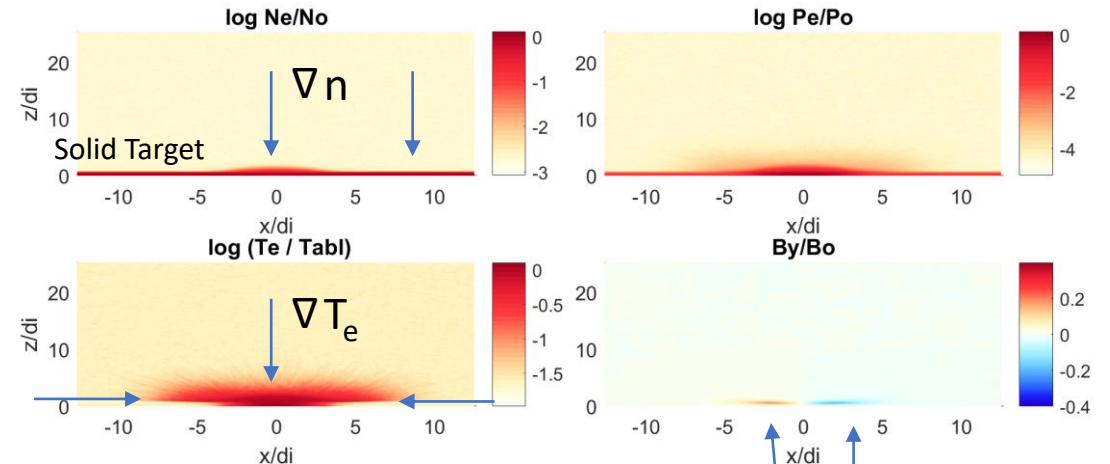
$$\frac{\partial \mathbf{B}}{\partial t} = \nabla \frac{1}{n_e e} \times \nabla p$$

$$\frac{\partial \mathbf{B}}{\partial t} = -\frac{1}{n_e e} \nabla n_e \times \nabla T_e$$



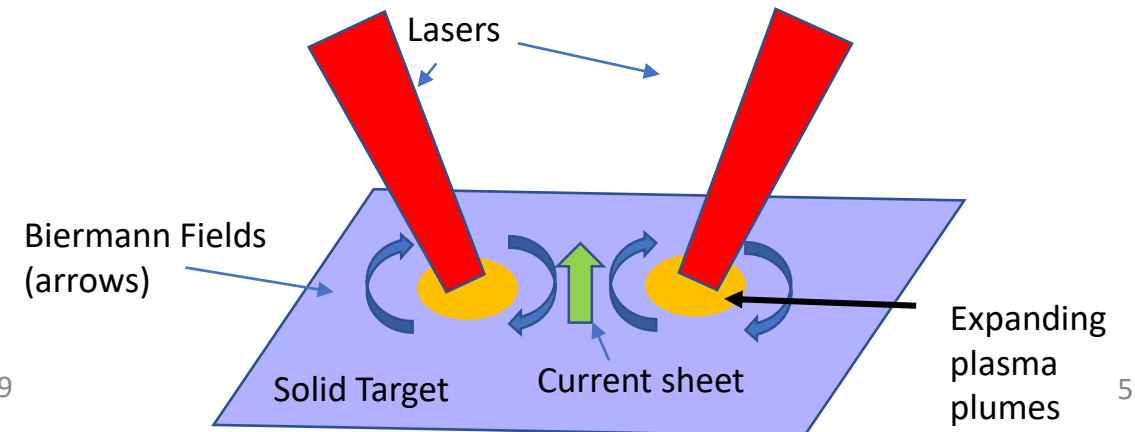
Example PIC Simulation Plasma Profiles **EARLY TIME:**

$t/t_d = 0.537$



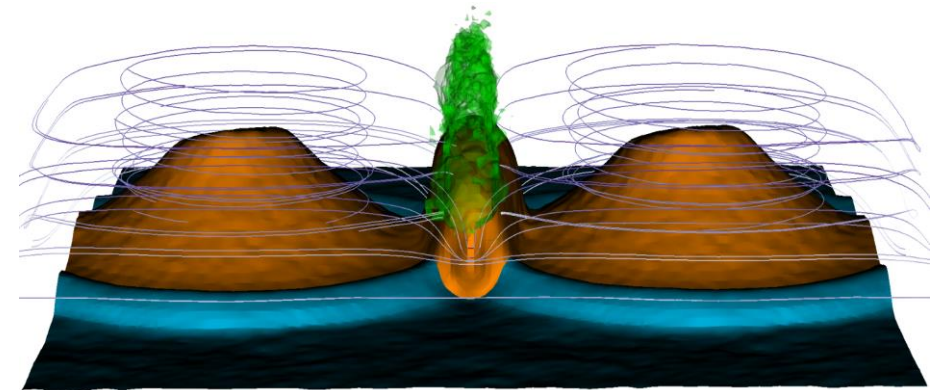
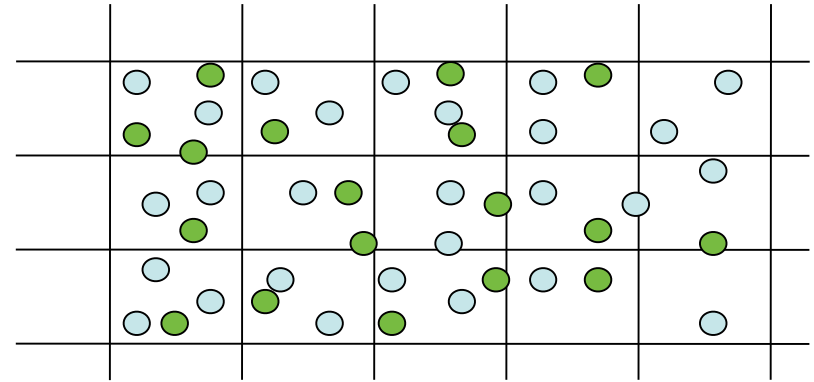
Biermann fields about expanding plume

Experimental Scenario



We use PSC, a fully kinetic, relativistic particle-in-cell code

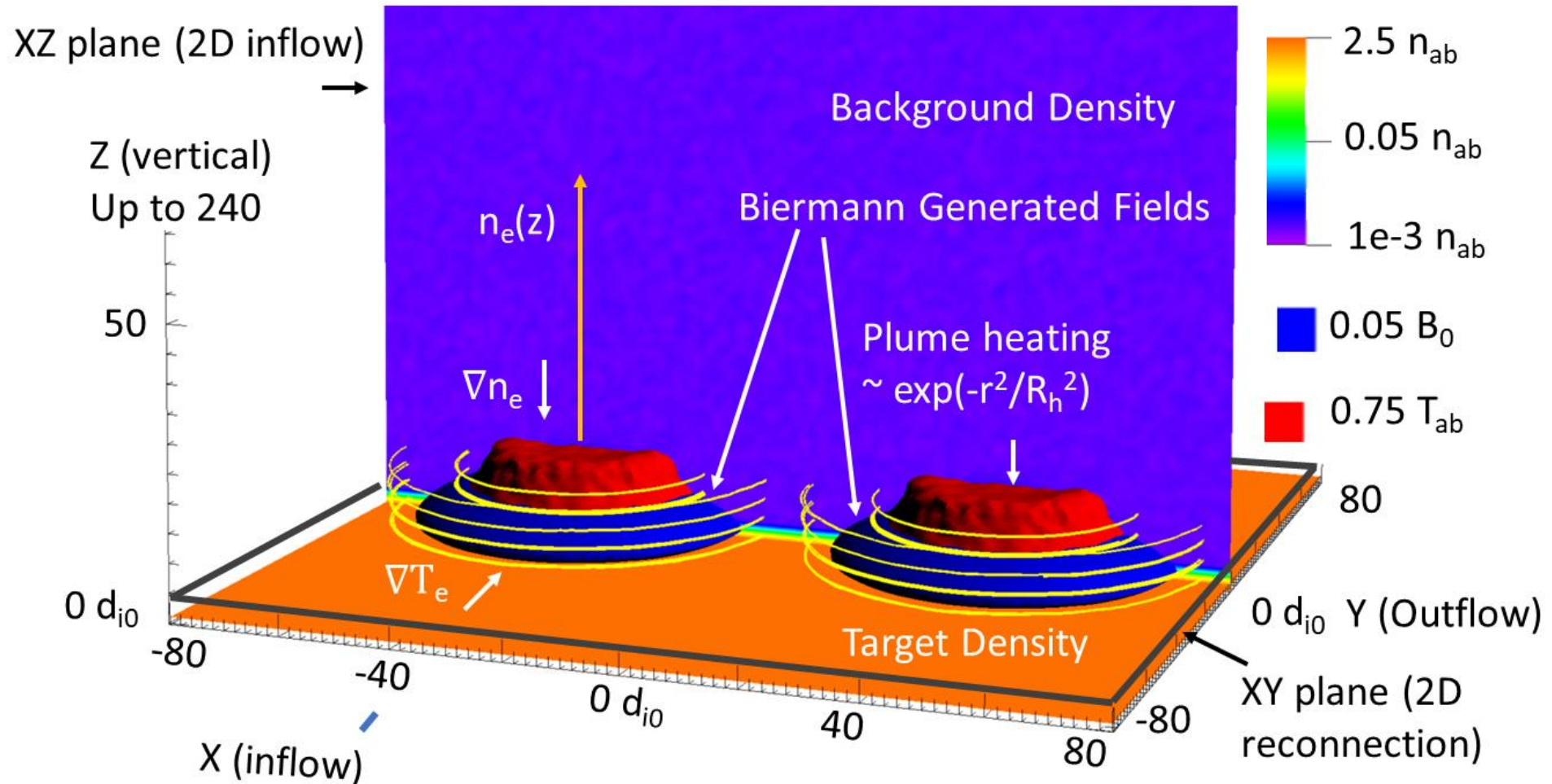
- Explicit, full-F pic code.
- Quasi-particles approximate particle distribution function
- Solves discretized Maxwell's equations and particles EOM:
 - Yee's grid discretization, finite difference time domain solver
 - particles EOM integrated using Boris scheme
 - 1st and 2nd order particle shapes available
- Includes binary Coulomb collision operator
- Efficient load balancing for massive parallel simulations
- Kinetic simulations can capture novel kinetic effects within HED plasma experiments
- Represents a new platform for studying HED experiments



Novel 3-D Particle in Cell Simulations capturing field generation through reconnection

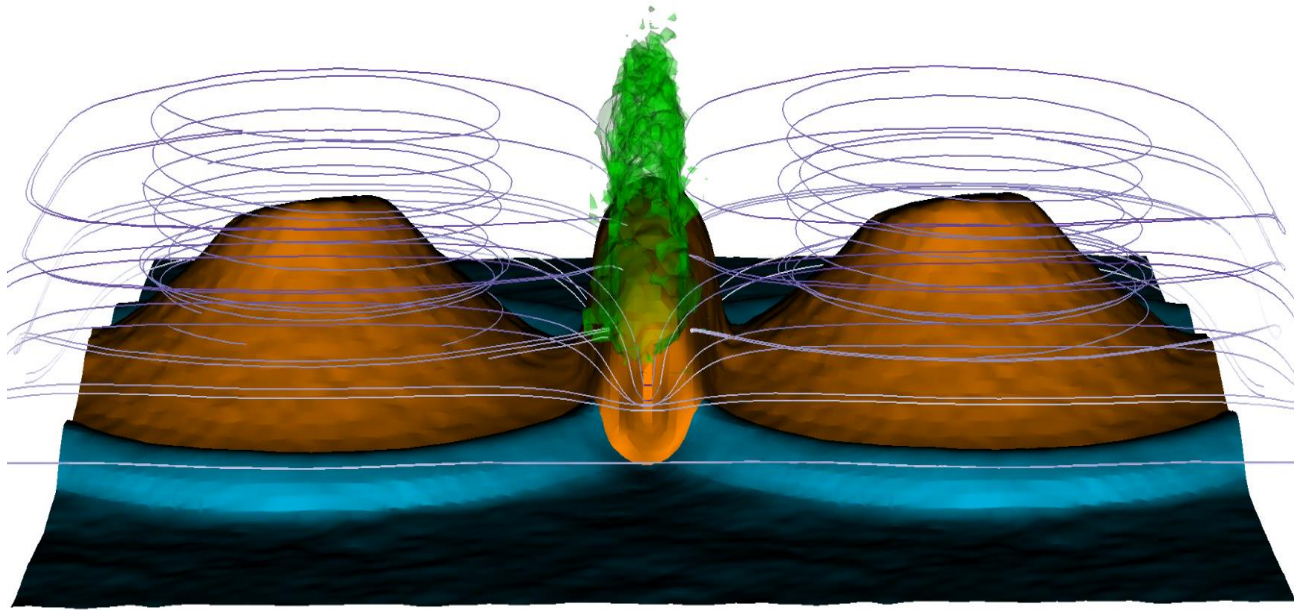
- Laser approximated by random electron heating $e^{-(r/rc)^k}$ within target
- n_e ablation profile along the vertical ablation matches well to rad-hydro simulations.

3-D Simulation Setup

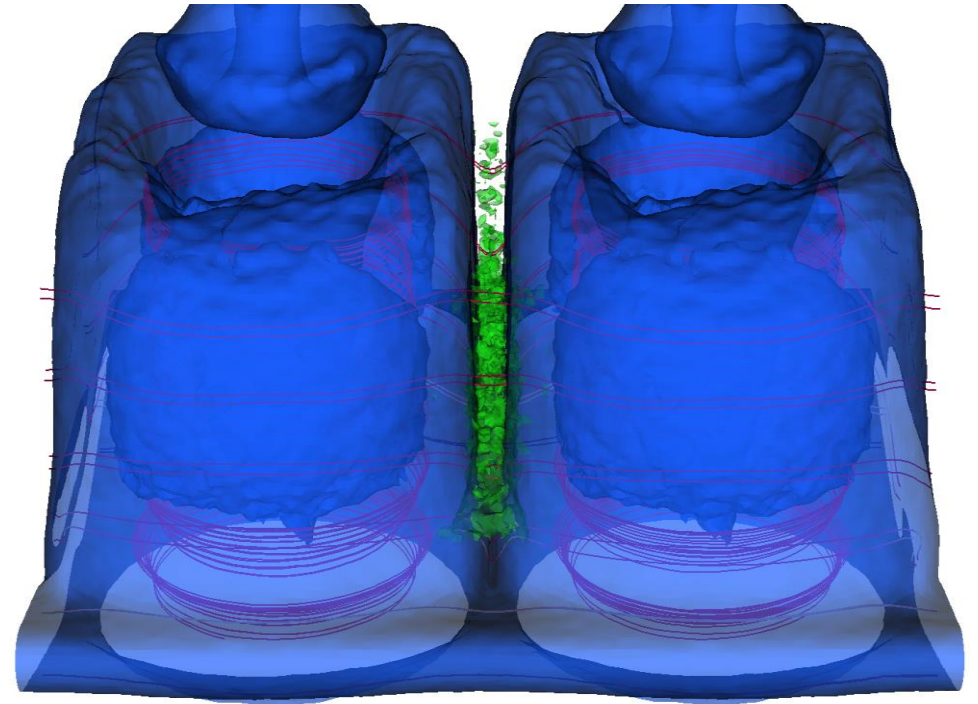


3-D simulations show dynamic, spatially dependent magnetic reconnection

Two snapshots of current sheet evolution at the SG-II scale

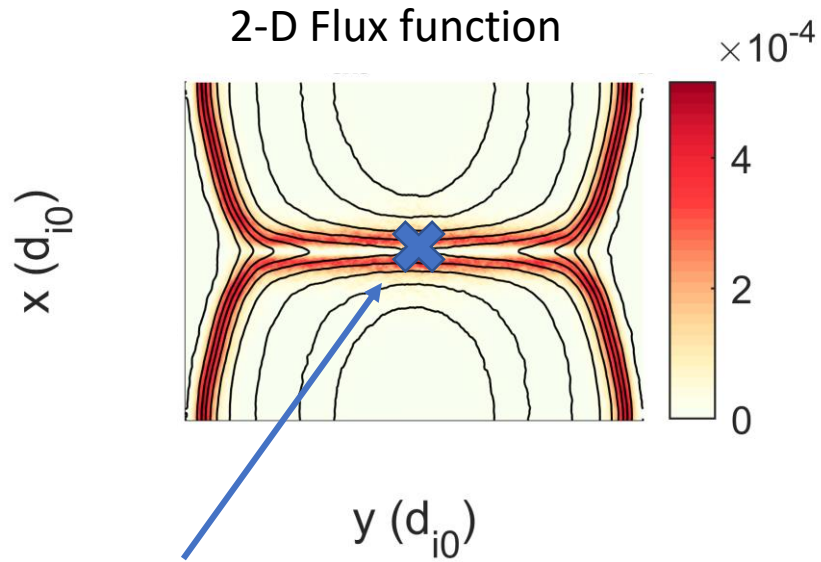


Orange shows electron pressure contour
Cyan shows density
Green shows $E \cdot J$



Blue shows B^2 contour
Green shows $E \cdot J$

Connections to 2-D collisionless reconnection



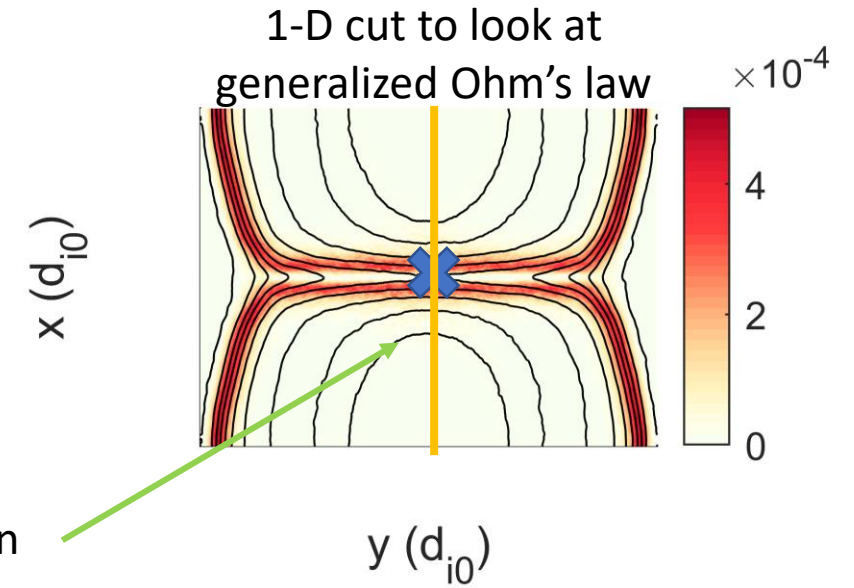
In 2-D, non-ideal electric field at the x-point yields reconnection rate.

Generalized Ohm's law typically shows the **traceless pressure tensor is typically responsible**

Also referred to as the non-gyrotropic pressure tensor

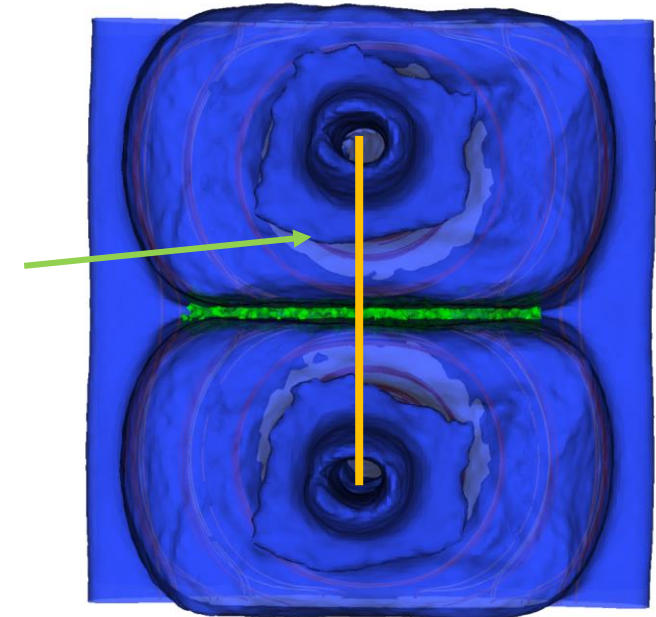
$$\mathbf{E} = -\mathbf{v} \times \mathbf{B} + \frac{\mathbf{j} \times \mathbf{B}}{n_e e} - \frac{\nabla p_e}{n_e e} - \frac{\nabla \cdot \Pi_e}{n_e e} + \frac{\mathbf{R}_{ei}}{n_e e},$$

APS DPP 2019

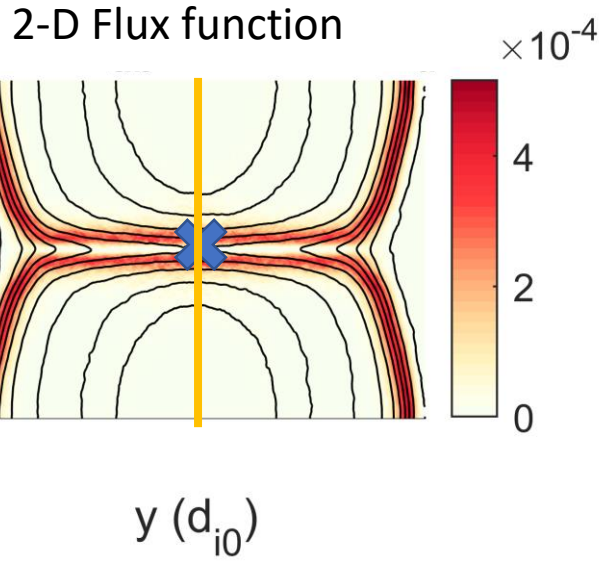


Next Slide: 1-D cuts along inflow (orange) direction and look at generalized Ohm's law to understand reconnection

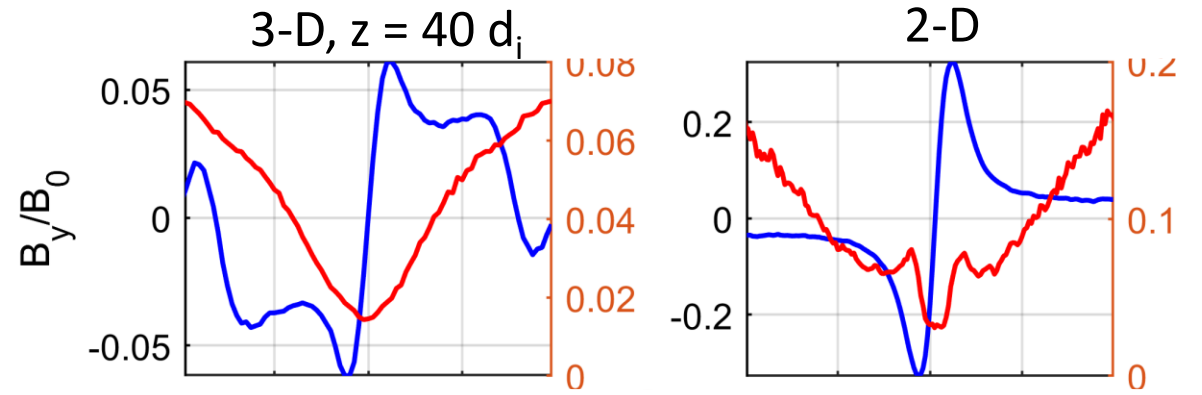
In 3-D, we take 1-D cuts at various vertical locations



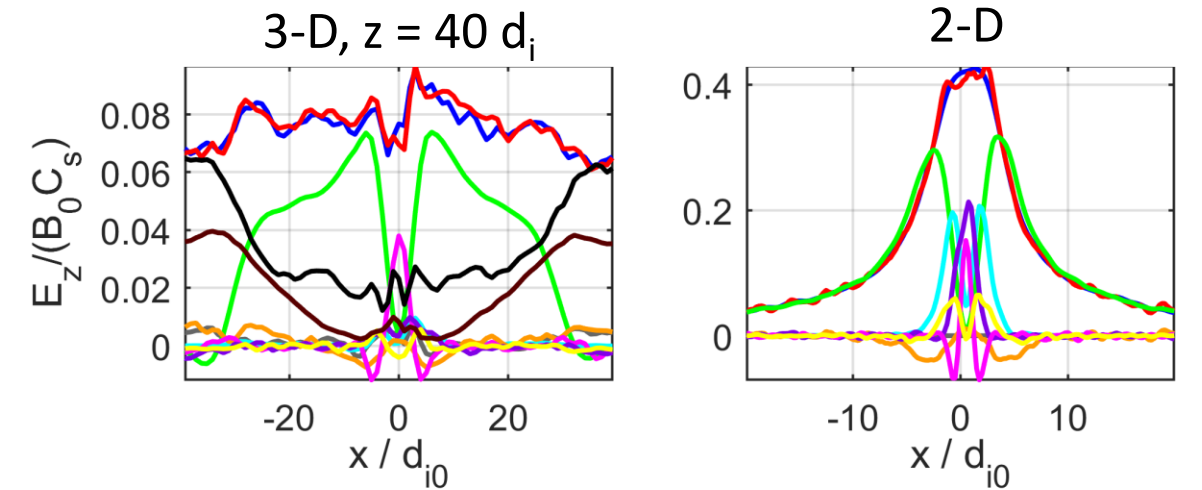
Traceless Pressure tensor plays significant role in both 2-D and 3-D reconnection



Magnetic field Profiles



Generalized Ohm's law



$$\mathbf{E} = \underbrace{-\mathbf{v} \times \mathbf{B}}_{\text{red}} + \underbrace{\frac{\mathbf{j} \times \mathbf{B}}{n_e e}}_{\text{green}} - \underbrace{\frac{\nabla p_e}{n_e e}}_{\text{black}} - \underbrace{\frac{\nabla \cdot \Pi_e}{n_e e}}_{\text{purple}} + \underbrace{\frac{R_{ei}}{n_e e}}_{\text{yellow}}$$

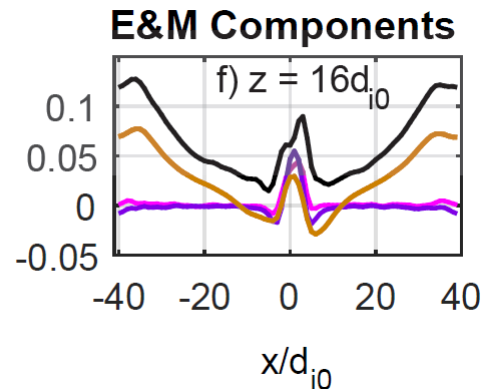
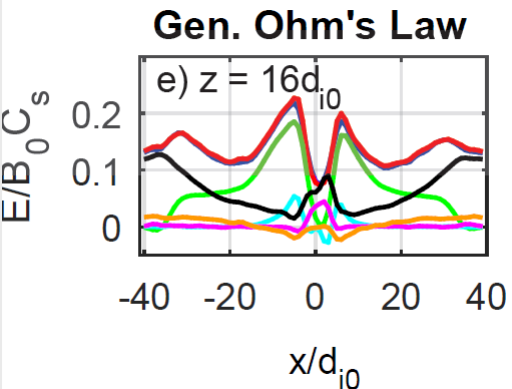
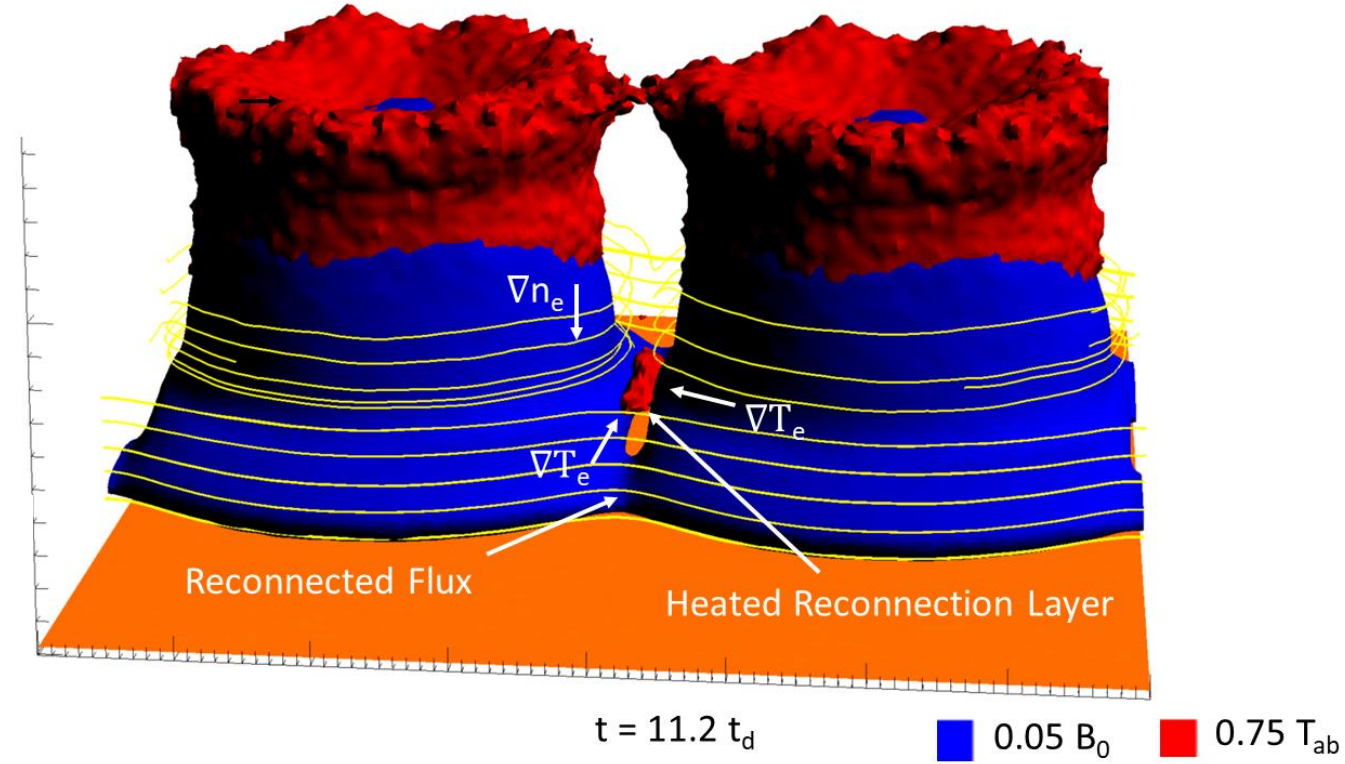
Purple and magenta show different components of the traceless pressure tensor- significant in 2-D and 3-D

New Reconnection mechanism: Biermann Battery mediated Reconnection

- Current sheet gets heated during reconnection
 - This reverses temperature gradient!
- Density gradient remains pointed toward target.
- Biermann cross-product reverses, leading to Biermann reconnection
- This process contributes to roughly 30% of the reconnection

$$E = -v \times B + \frac{j \times B}{n_e e} - \frac{\nabla p_e}{n_e e} - \frac{\nabla \cdot \Pi_e}{n_e e} + \frac{R_{ei}}{n_e e}$$

Visualization of Biermann-mediated Reconnection

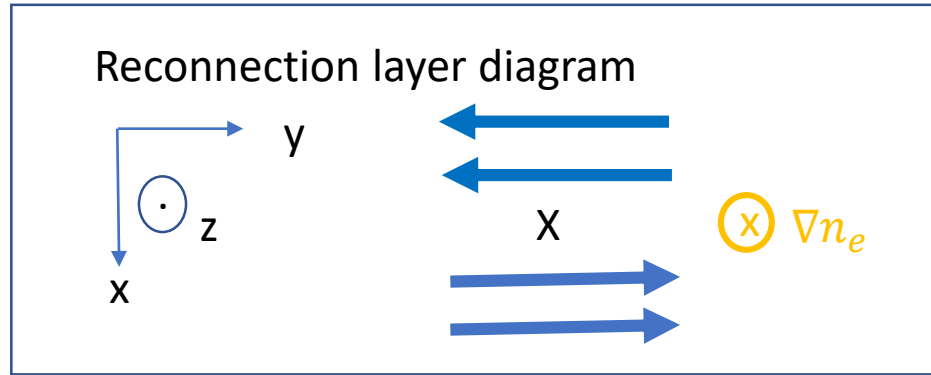


Black = ∇p_e
 Brown = $\nabla p_{e,em}$

J. Matteucci, W. Fox, A. Bhattacharjee, D. B. Schaeffer, C. Moissard, K. Germaschewski, G. Fiksel, and S. X. Hu, Phys. Rev. Lett. **121**, 095001 (2018)

Biermann Battery mediated Reconnection could be important in space physics!

$$\mathbf{E} = -\mathbf{v} \times \mathbf{B} + \frac{\mathbf{j} \times \mathbf{B}}{n_e e} - \frac{\nabla p_e}{n_e e} - \frac{\nabla \cdot \Pi_e}{n_e e} + \frac{\mathbf{R}_{ei}}{n_e e},$$



Assume out of plane ∇n_e and inflow T_e dependence

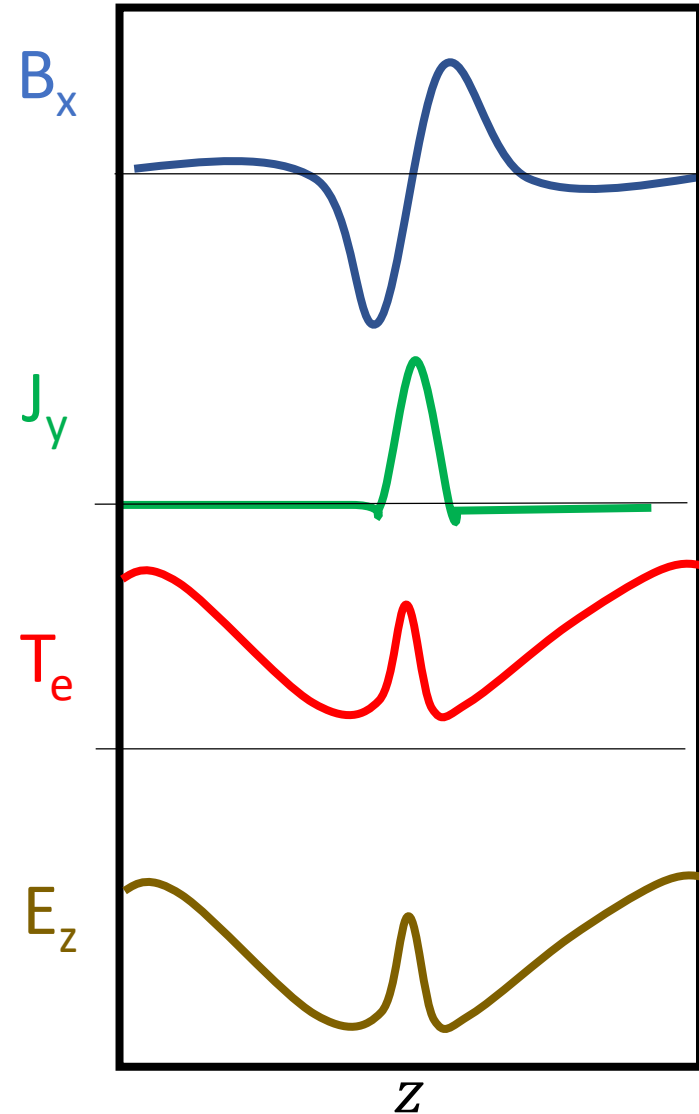
$$E_z(x, y=0, z_0) = T_e(x) / eL_n \quad R_{\text{Biermann}} \approx \frac{\delta_{\text{rec}} T_e}{eL_T L_n B_{\text{up}}^* V_A^*} = \frac{\beta_e}{2} \frac{\delta_{\text{rec}} d_{i,\text{rec}}}{L_T L_n}$$

Where $R_{\text{Fast reconnection}} \approx 0.1$

Example: turbulent magnetosheath (Retino, Nat Phys 2007)

$\beta \approx 1, \delta_{\text{rec}} \approx L_T, L_{n,\text{out of plane}} \approx 10 d_i$, where $d_i \approx 30 \text{ km}$, yielding $R_{\text{Biermann}} \approx 0.05$

Also observed in 3-D Two-Fluid 10-Moment Modeling of Ganymede's Magnetosphere (L. Wang, JGR 2018)

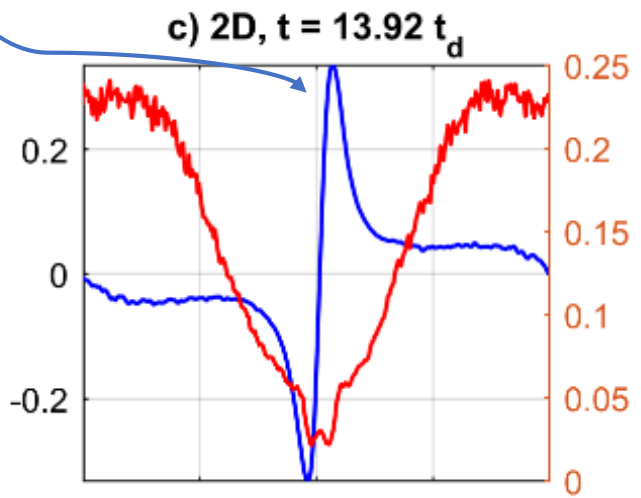
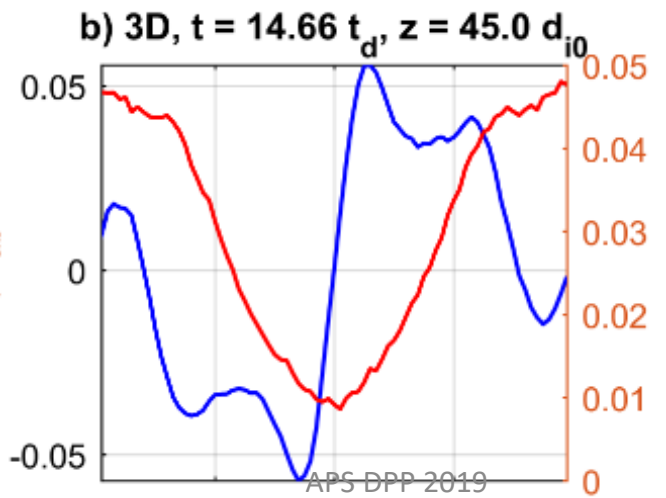
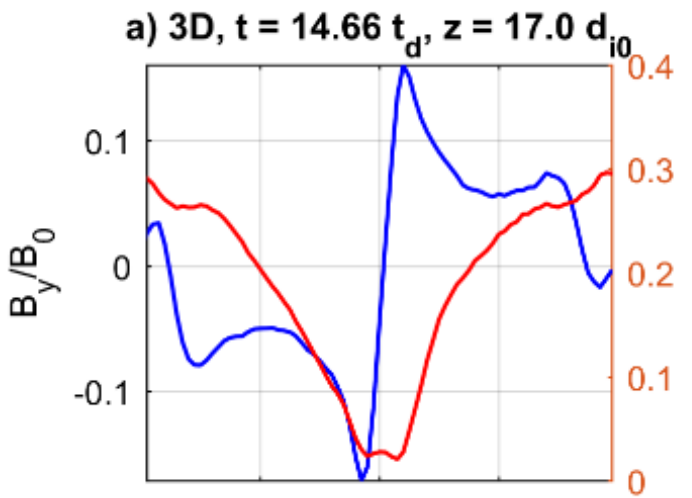
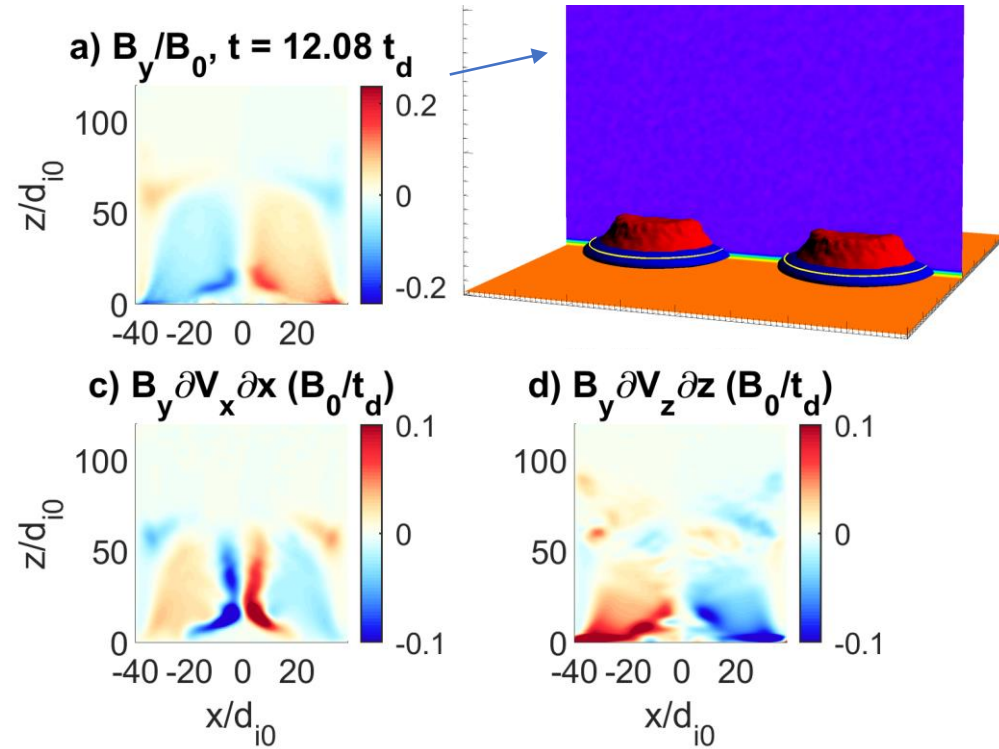


J. Matteucci, W. Fox, A. Bhattacharjee, D. B. Schaeffer, C. Moissard, K. Germaschewski, G. Fiksel, and S. X. Hu, Phys. Rev. Lett. **121**, 095001 (2018)

Flux Dilution reduces reconnection layer compression, reducing inflow B-field

- Flux pile-up in reconnection layer observed in 2-D (Fox PRL 2011).
- Speeds up fast reconnection ($0.1 B_{up} V_A$)!
- In 3-D, we see no flux pile-up!
-Dilation of field in the out of plane direction
- Purely due to $\partial_t B = \nabla \times (V \times B)$

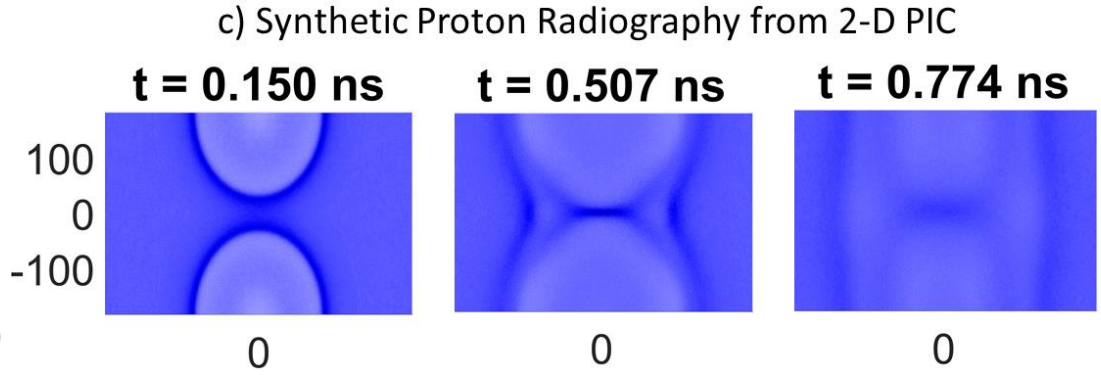
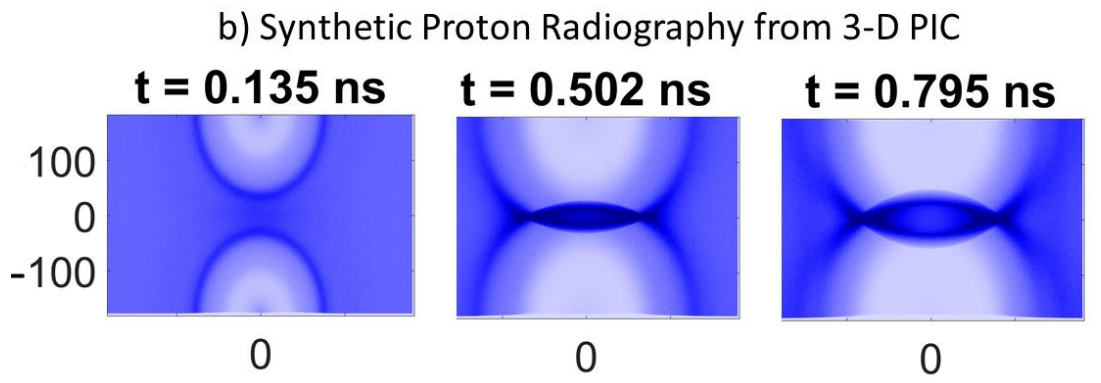
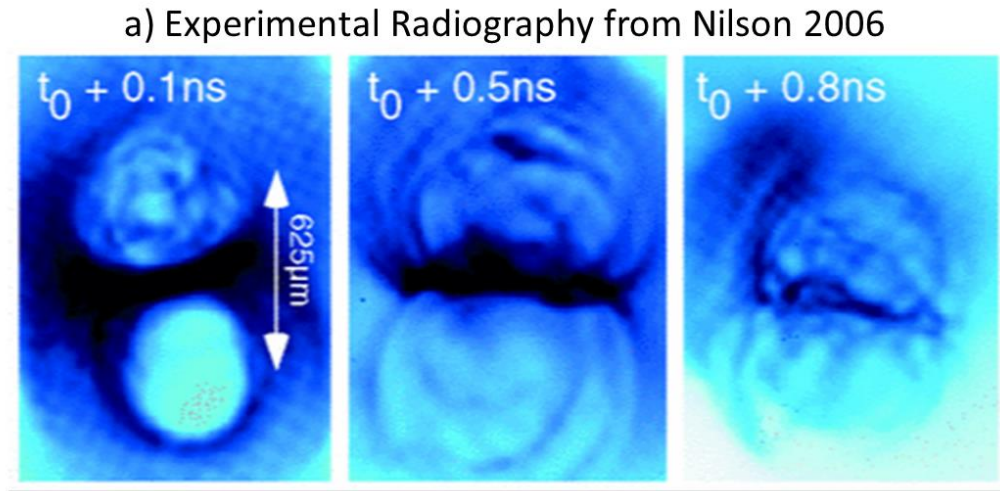
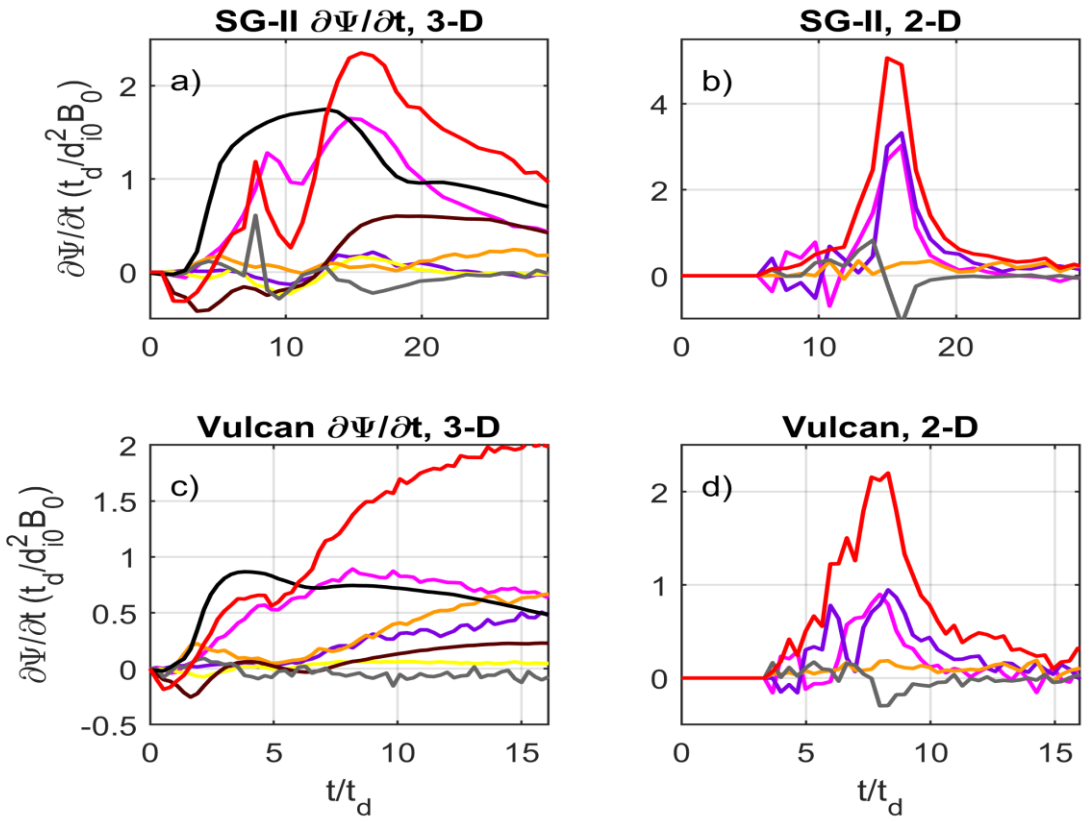
3-D vs. 2-D reconnection layer B-field profiles



Reconnection proceeds faster in 2-D due to compression of reconnection layer

- Compression in 2-D leads to faster reconnection rates, which scale roughly as $B_{up} V_A$
- Global reconnection in 2-D can proceed 2x faster than in 3-D

Red shows global reconnection,
 Brown shows Biermann Reconnection
 Purple and magenta show Traceless Pressure Reconnection

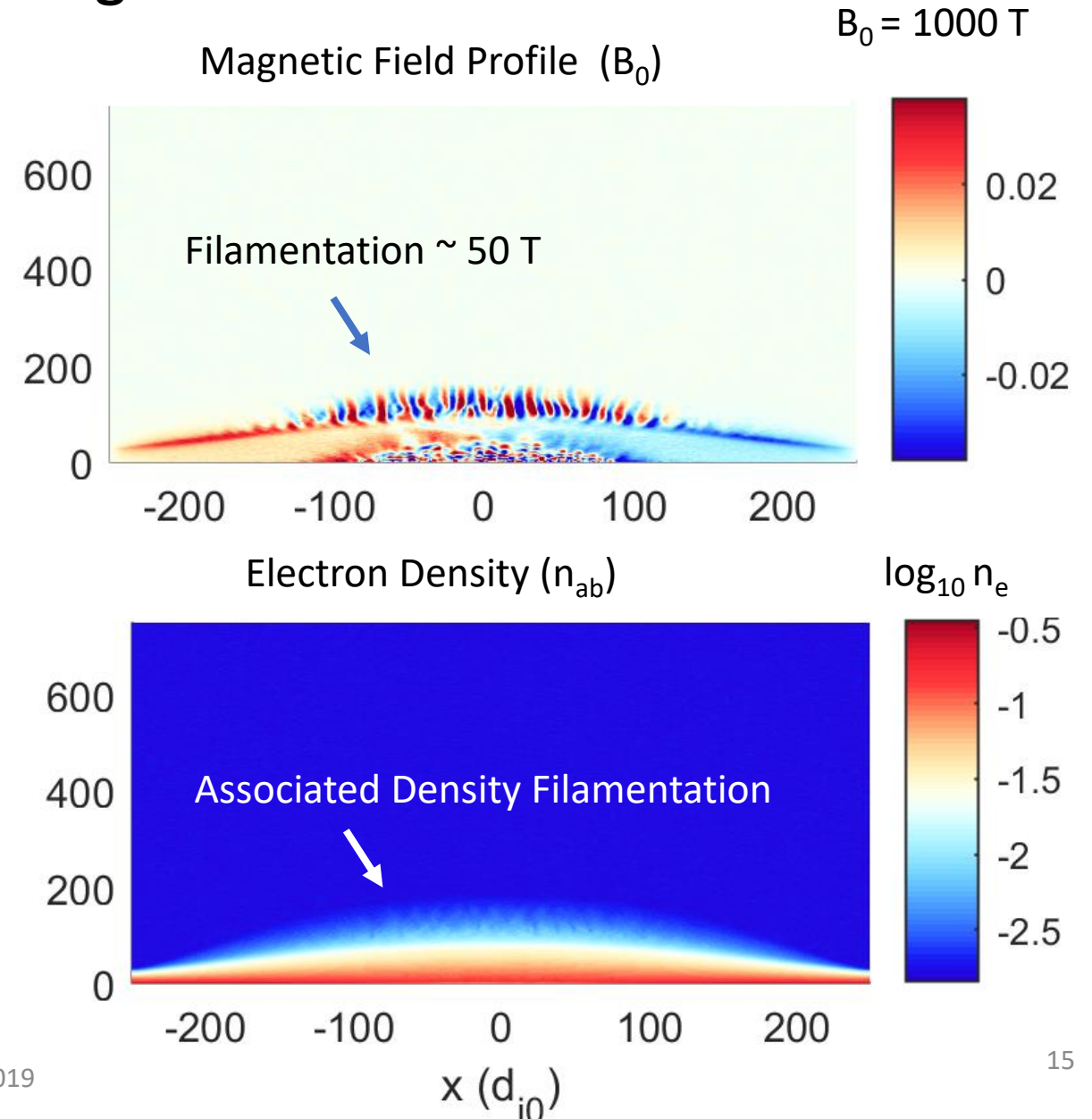


Current NIF and Omega EP campaigns provide impetus to go to larger scales: We find filamentary magnetic field generation!

Current HED reconnection experiments seek a large separation scale between L (system size) and ion skin depth

For $L, R_h \gg d_i$:

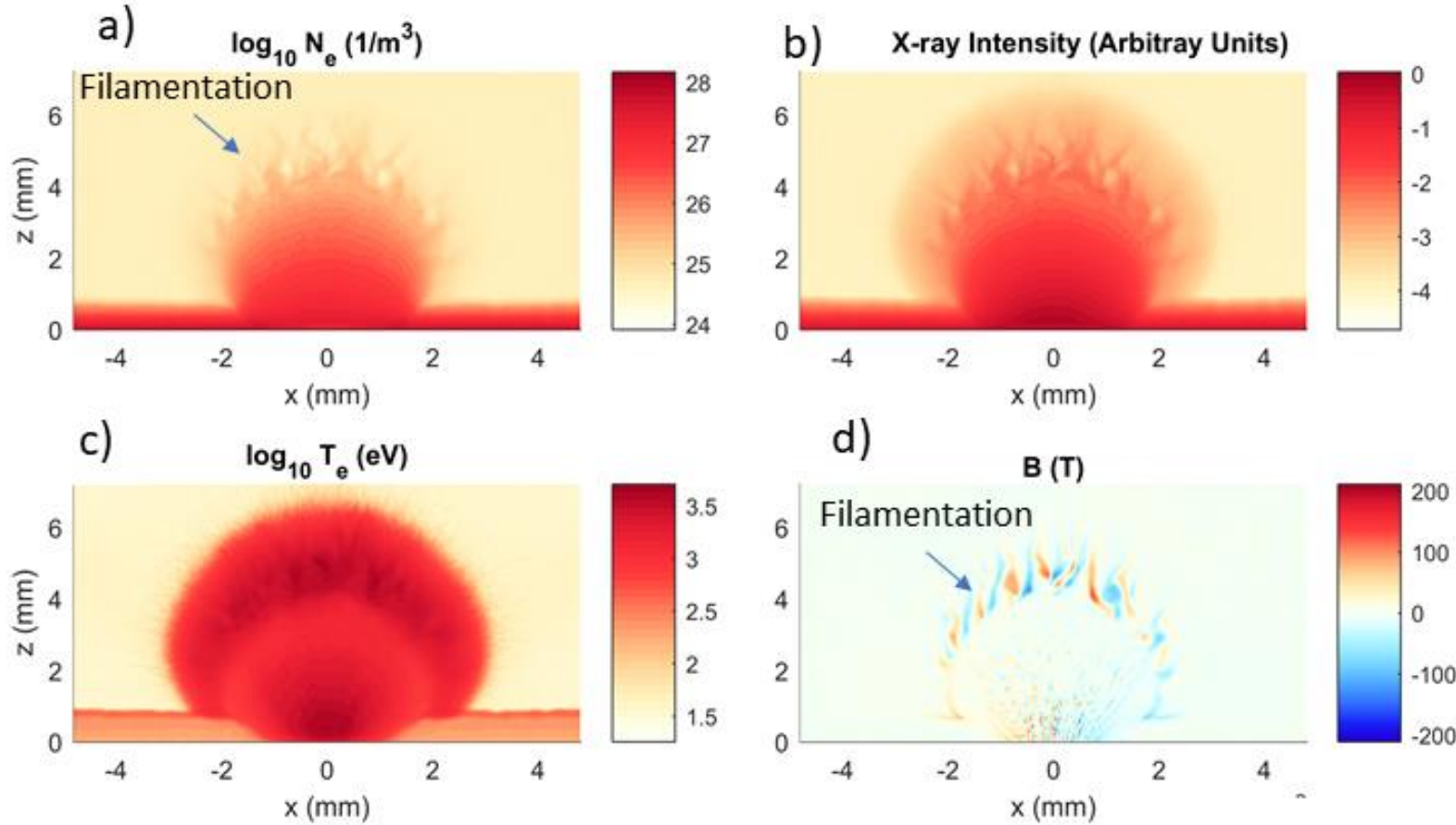
- We observe additional filamentary instability, out generating Biermann, producing 50 T fields and associated density oscillations
- Filamentation would be important in reconnection experiments as well as hohlraums.



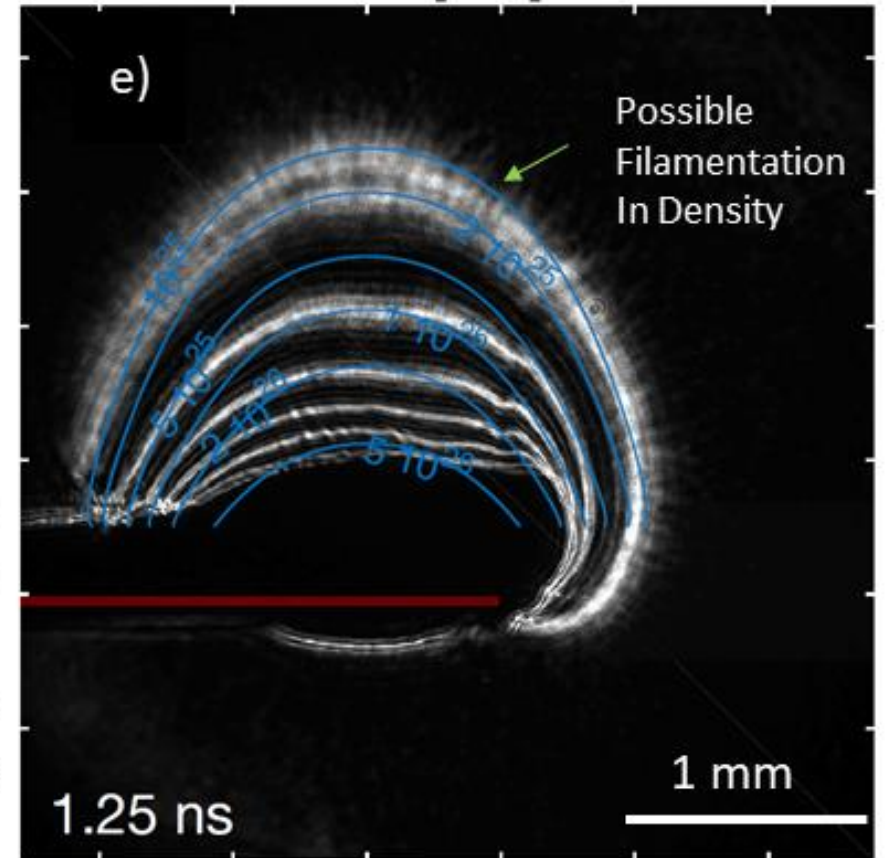
We observe filamentation in the experiments as well, similar to simulations!

PIC Simulation of NIF expanding into background plasma

t = 2.2 ns



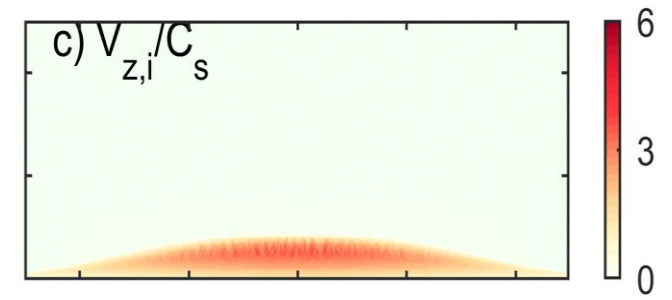
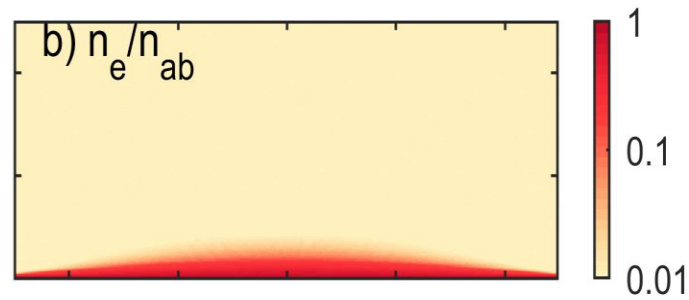
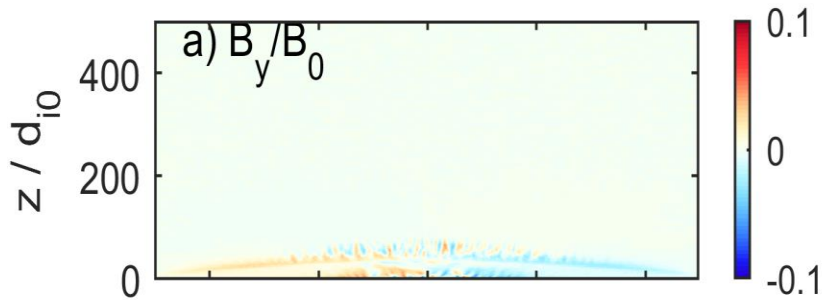
Refractometry from EP, single plume



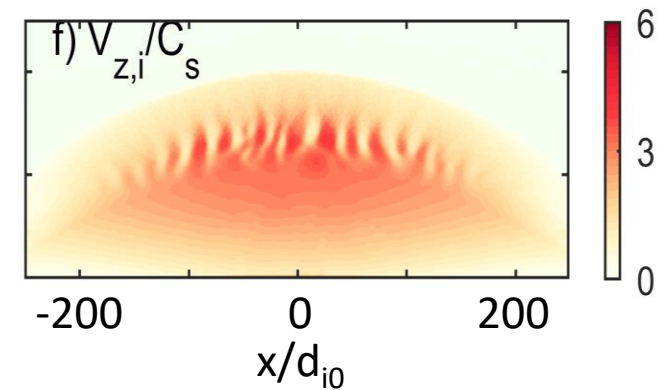
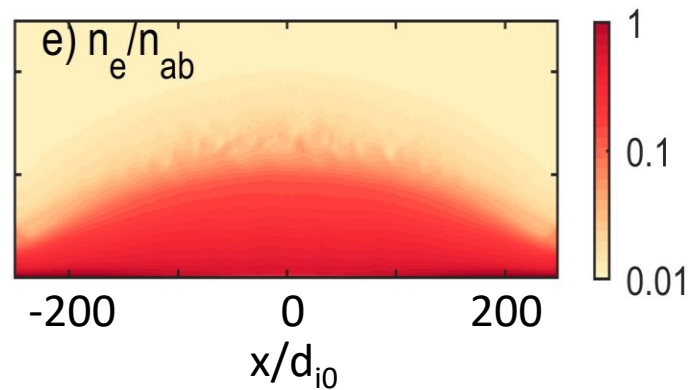
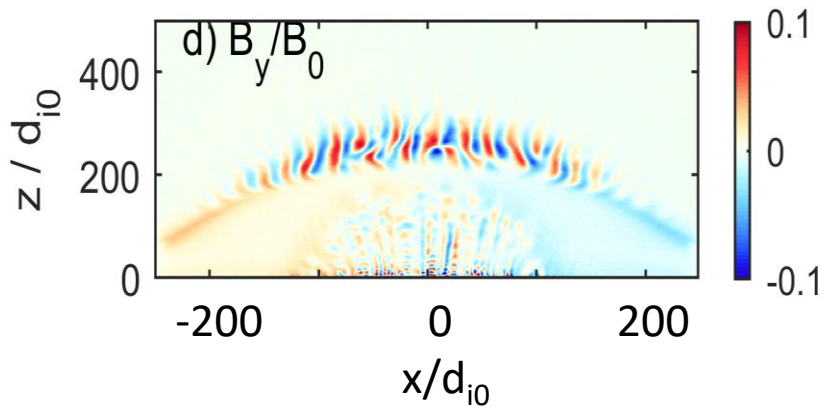
Filamentation appears in ablation corona, where ablation ions interact with background ions

- Possible counterstreaming between ablation ions and background ions
- Counterstreaming is known to drive the Weibel instability

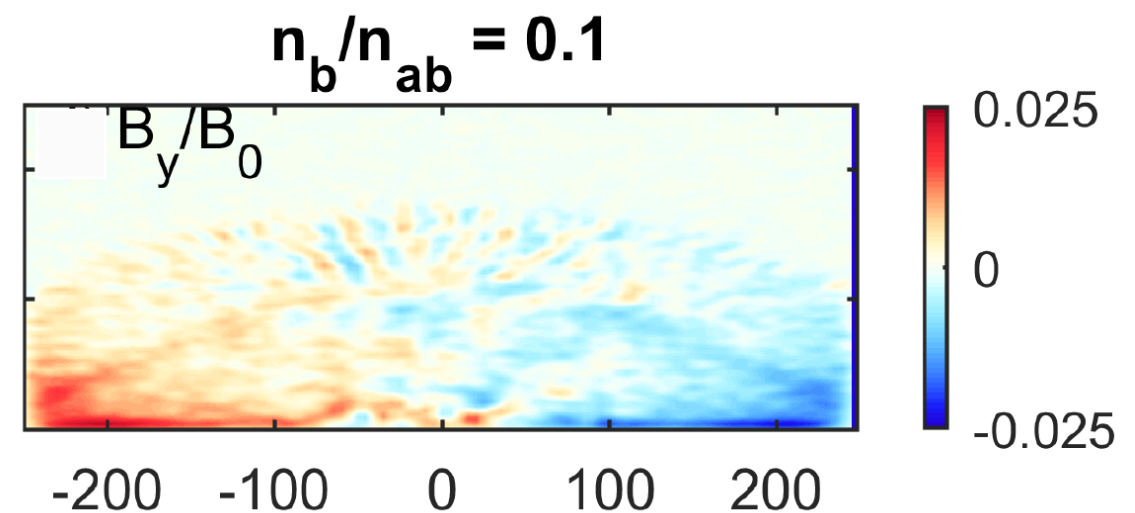
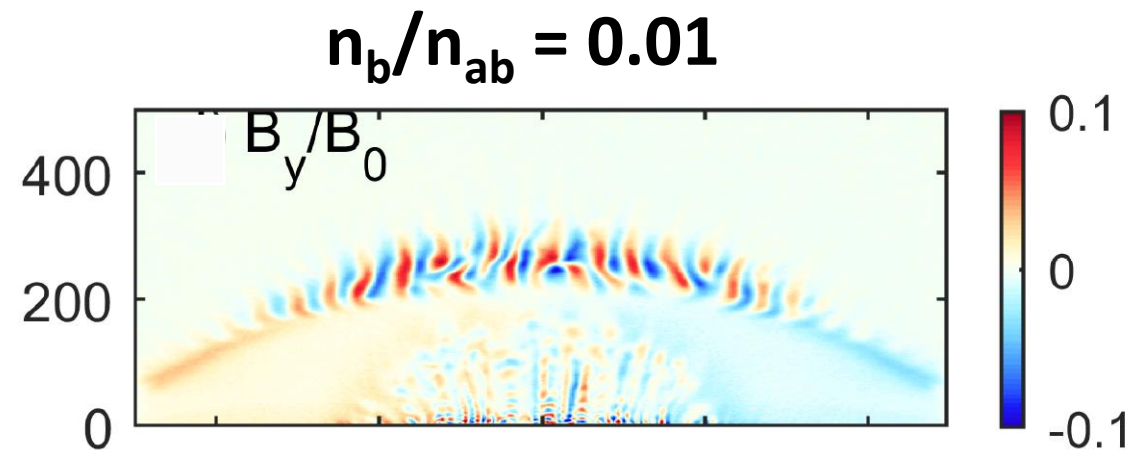
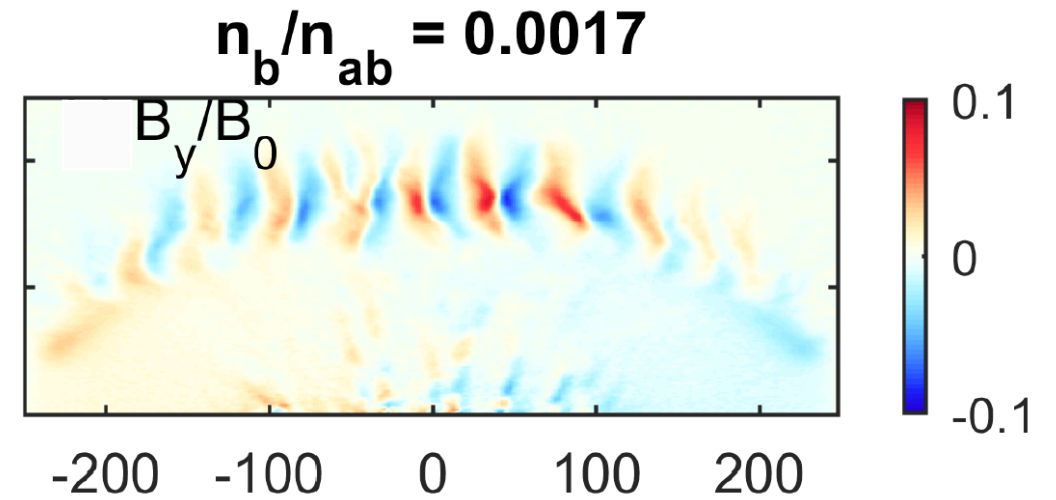
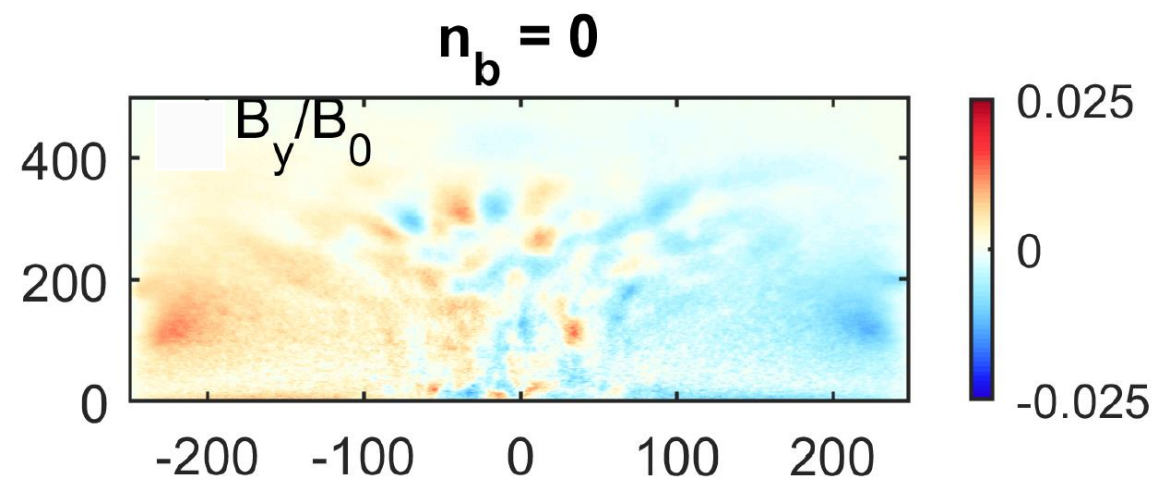
$t/t_d = 16.57$



$t/t_d = 74.58$



Filamentation appears to depend on background density both in wavelength and in saturation values



Potential instability origin: Counter-streaming between background and ablation ions

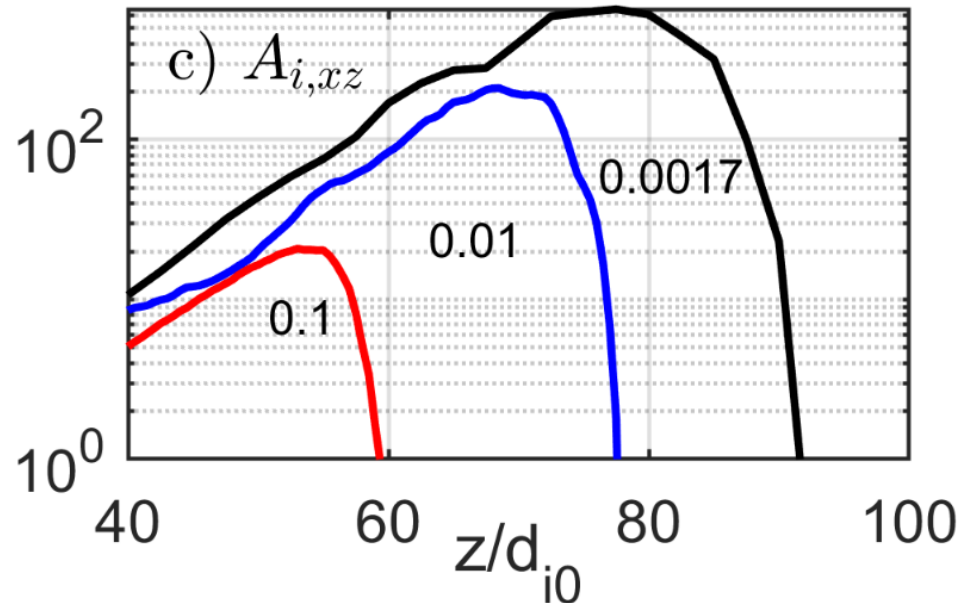
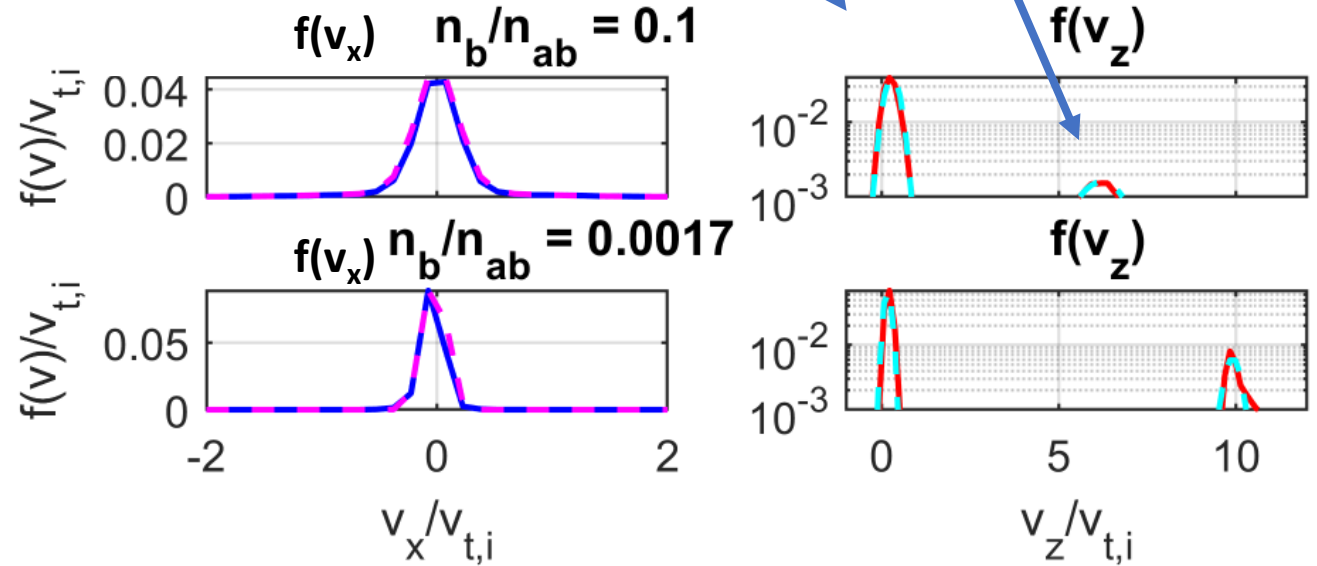
We find large relative counter-streaming between ablation ion and background ions

This drives Weibel instability, through the effective temperature anisotropy:

$$A_i = T_{zz,i}/T_{xx,i} - 1$$

Where $T_{zz,i} = \int f(v_z) (v_z - v_{z0})^2 dv_z$

Ion Velocity distribution functions w/ fits in dashed lines



We find A_i depends greatly on the background density n_b
 This follows from a simple ablation analysis where: $V_z(z) = C_s(1 + z/tC_s)$

We expect this to impact the growth rates if A_i is the origin of the instability.

Growth rates show quantitative agreement with linear ion-driven Weibel instability dispersion relations

We track the growth of the B-field filaments as a function of background density

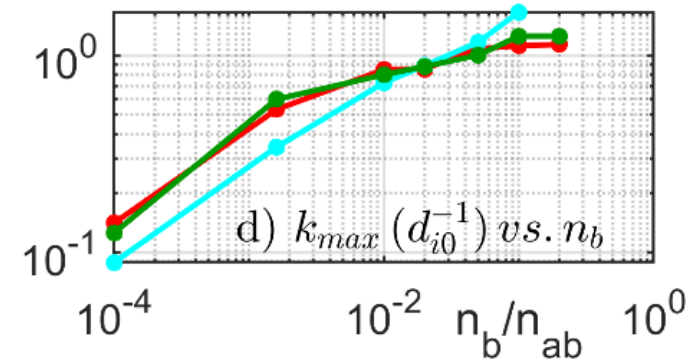
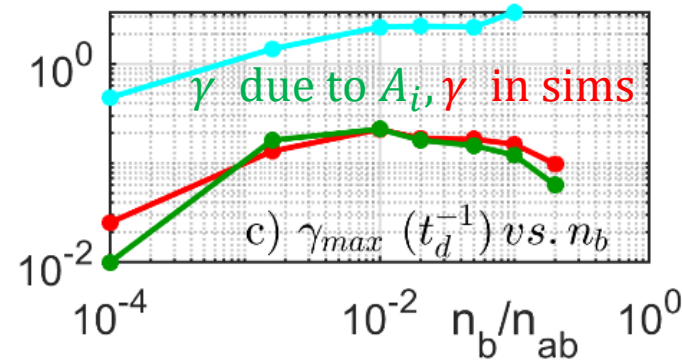
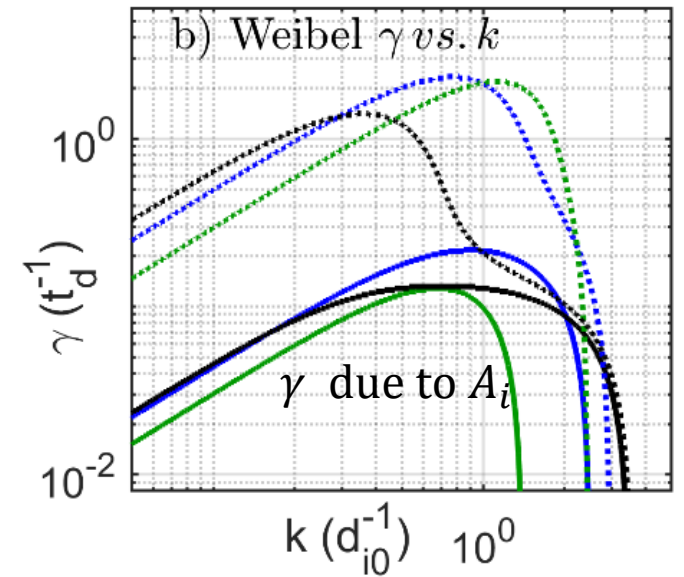
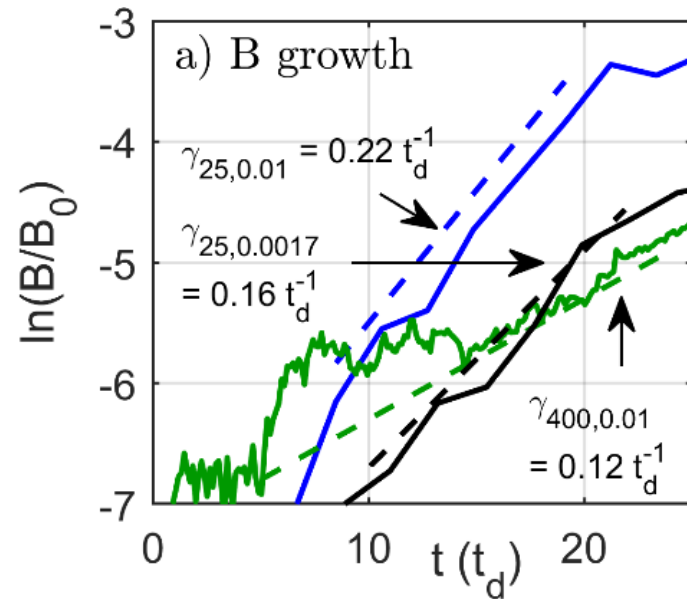
By using A_i from our simulations, we can solve the Weibel dispersion relation:

$$0 = c^2 k^2 - \omega_k^2 - \sum_s \omega_{p,s}^2 [A_s] - \sum_s \omega_{p,s}^2 [A_s + 1] \xi_s Z(\xi_s)$$

$$\xi_s = \omega_k / (k v_{th,\parallel})$$

We compare the max growth rates vs. the measured growth rates vs. n_b

Finding excellent agreement with the Weibel instability driven by A_i



Density Oscillations grow linearly with B-field

B-field saturates around 50 T over $0.0017 - 0.05 n_b$

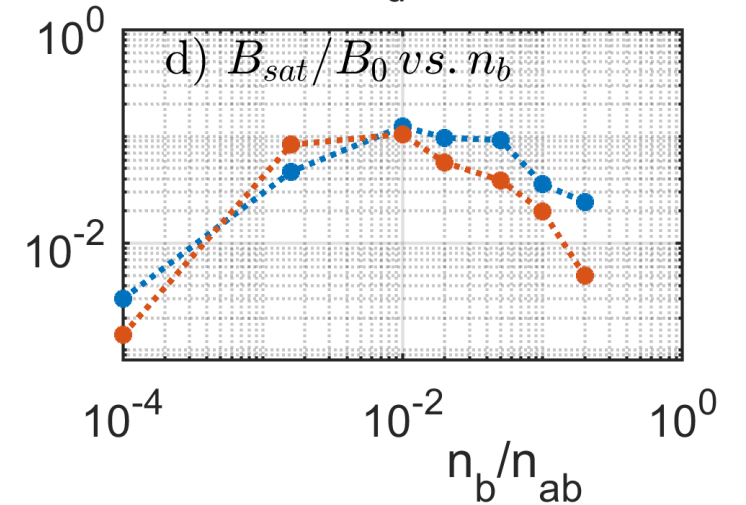
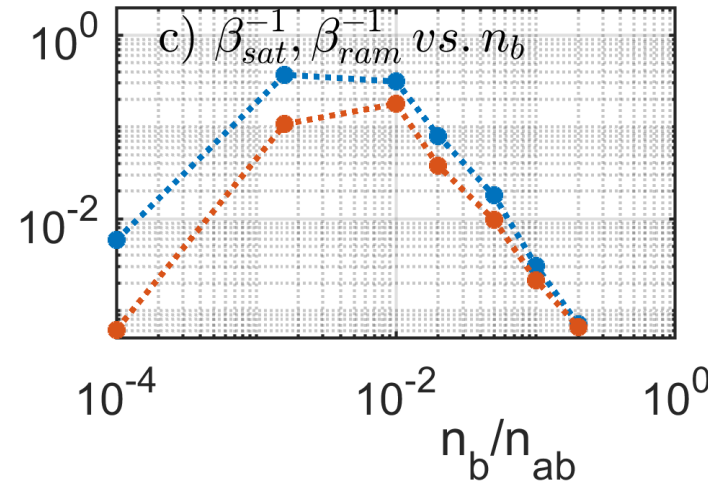
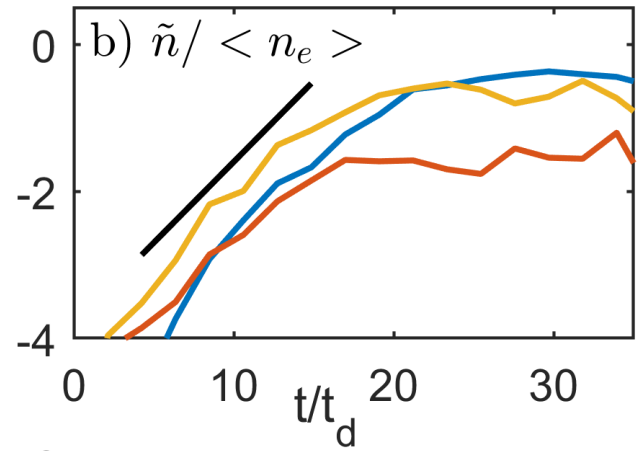
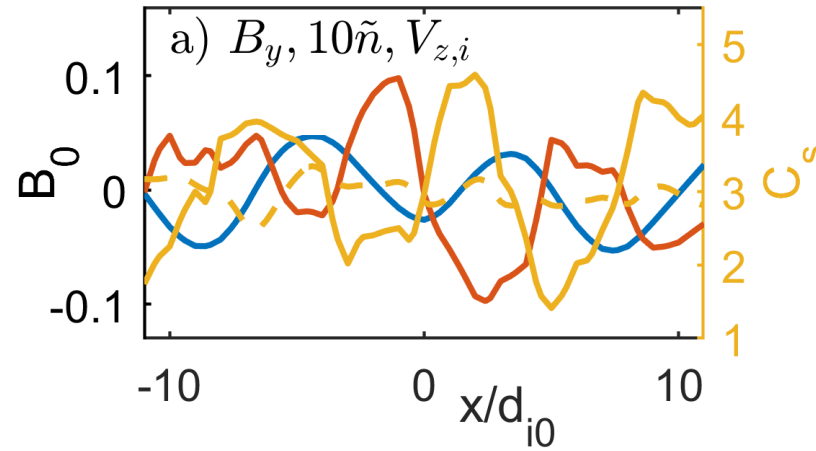
We find **density oscillations** grow linearly with **B-field filamentation** and **ion velocity perturbations**.

We observe saturated density oscillations at $0.01 n_{ab}$, corresponds to $2.3 \times 10^{25} \text{ m}^{-3}$.

B-fields saturate according to when initial growth rate \approx bounce frequency of ions: $\omega_{b,i} = \sqrt{kV_y B}$

We find significant filamentation (50 T) over a range of $0.0017 - 0.05 n_b$

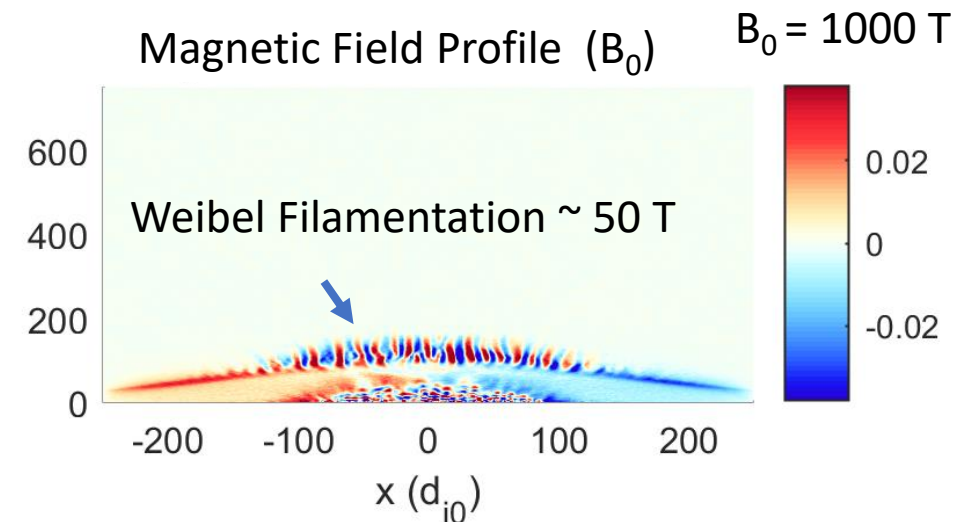
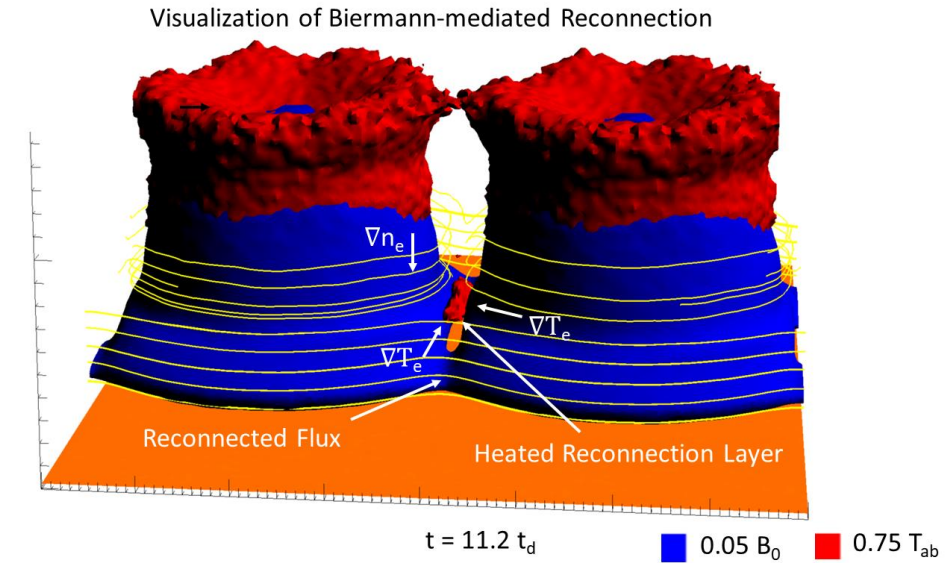
This is particularly relevant to hohlraum conditions where a fill gas of $\sim 4.5 \times 10^{25} \text{ m}^{-3}$ is frequently used.



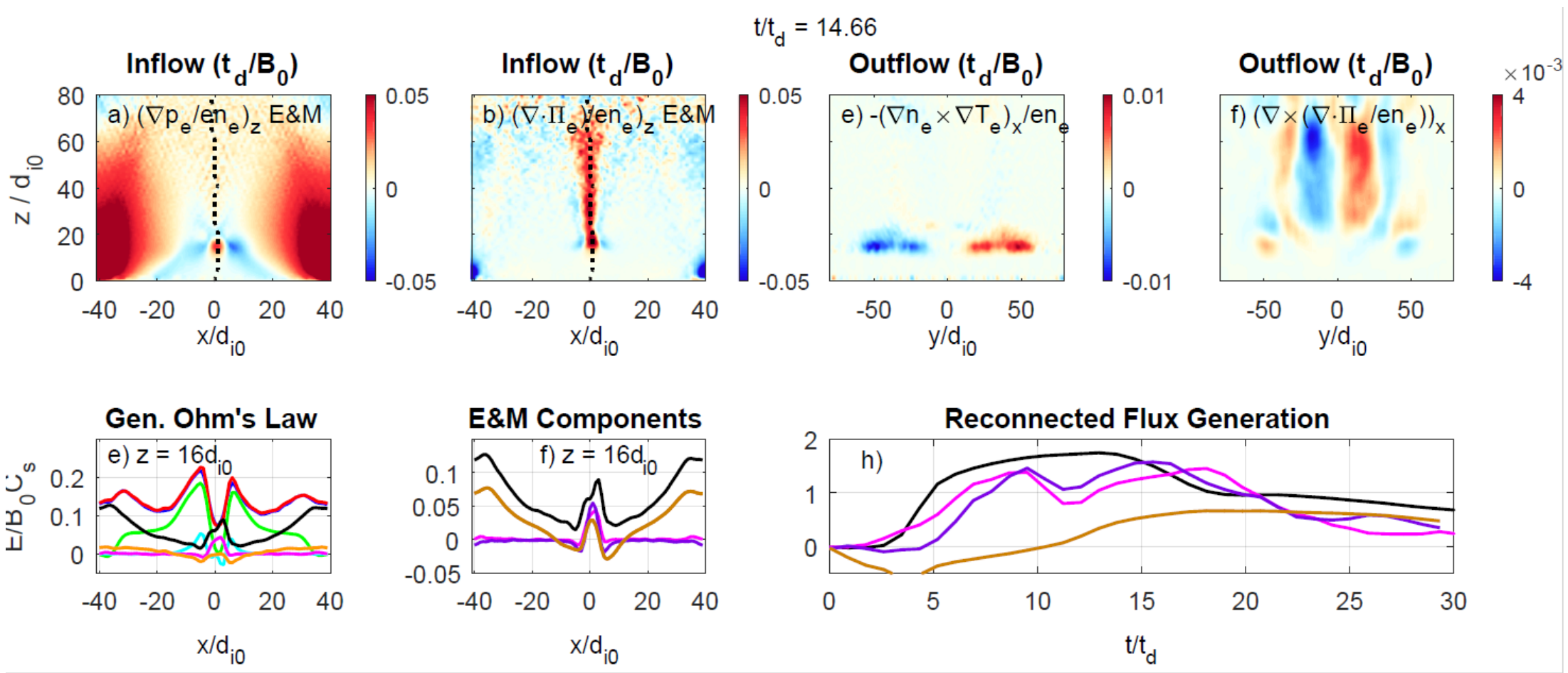
$$B_{ram} = \text{Flow Energy} / \text{Magnetic Energy}$$

Conclusions

- Full 3-D Kinetic simulations modeling self-consistent evolution of HED reconnection experiments.
- We observe a novel 3-D reconnection mechanism: **Biermann Battery reconnection** - could be relevant in space plasma.
- We find other 3-D modifications to HED reconnection experiments slowing down reconnection.
- In large 2-D ablation simulations, ion Weibel instability to drives generation of 50 -100 T fields and density oscillations.



Biermann Reconnection Backup



Comments:

- Importance of what I've done: first kinetic simulations
- Enjoy reconnection a bit more- show big energy figure- show pressure tensor for fast reconnection don't make that jump
- Transition to Weibel – make it smoother

Notes:

- Also, try to zoom out a little bit at the beginning to explain what is new and important about the capability
— fully kinetic simulations of plasma ablation, broad relevance to both “discovery experiments” and potentially hohlraums, etc.

In reconnection section, discuss some more ordinary reconnection aspects before launching into Biermann-mediation effect?

Remember, the audience will be more HEDP than reconnection, so they should get some more basic on reconnection.

- what are the necessary ingredients for reconnection?

- it may be worthwhile to show a simple 2-D reconnection sims first? There are many concepts - current sheet, inflows, rate, geometry, etc...

then, the audience will appreciate what is new in 3-D better

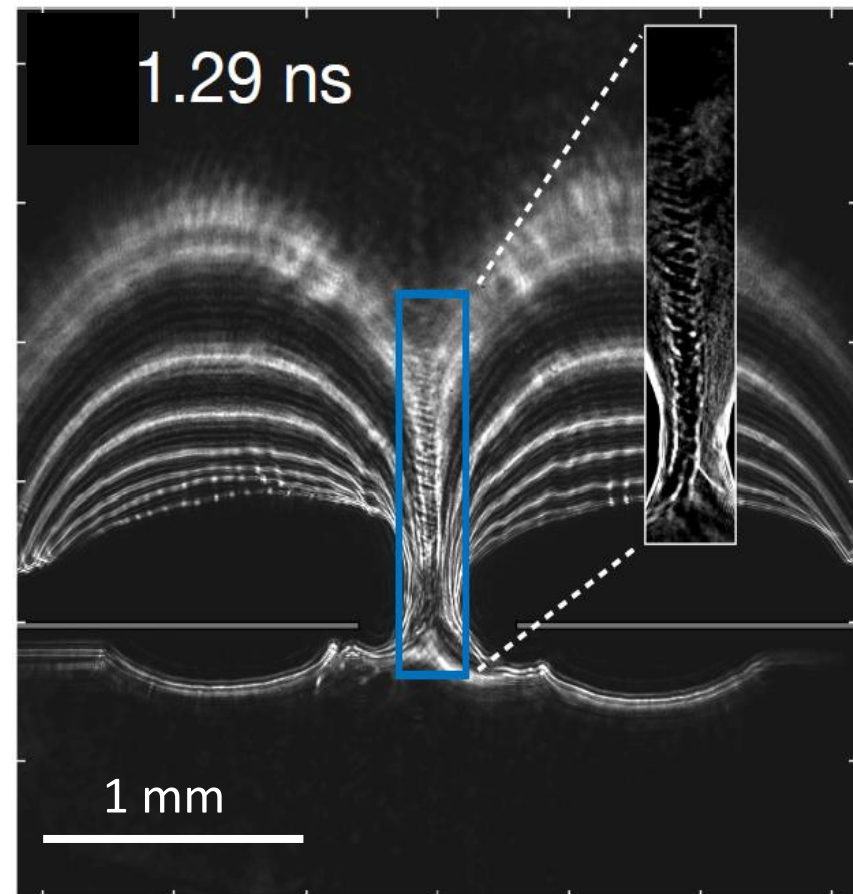
Make a bridge from the reconnection section to Weibel. Maybe something like, “EP and NIF experiments provided an impetus to do reconnection simulations at much larger scale. Turns out we find this other new physics at large system size, etc?” Explain what is the main parameter difference between your Weibel section and reconnection (mainly L/d_i , yes?)

Small point, in Weibel section, need to explain how counter streaming leads to a “Tzzi”. Without some explanation, some people will wonder what is going on. After all, with the counterstreaming, the distribution function doesn’t have a simple temperature anymore. As we know, it really comes down to that Weibel doesn’t really care about the individual velocities, just the overall moment anisotropy, but that is non-trivial! The order is more like: 1) See counterstreaming, 2) aha! Could be Weibel, 3) Weibel dispersion, 4) driving term is $A_i = T_{zzi}/T_{xxi} - 1$ as driving term 5) find where that exists in results.

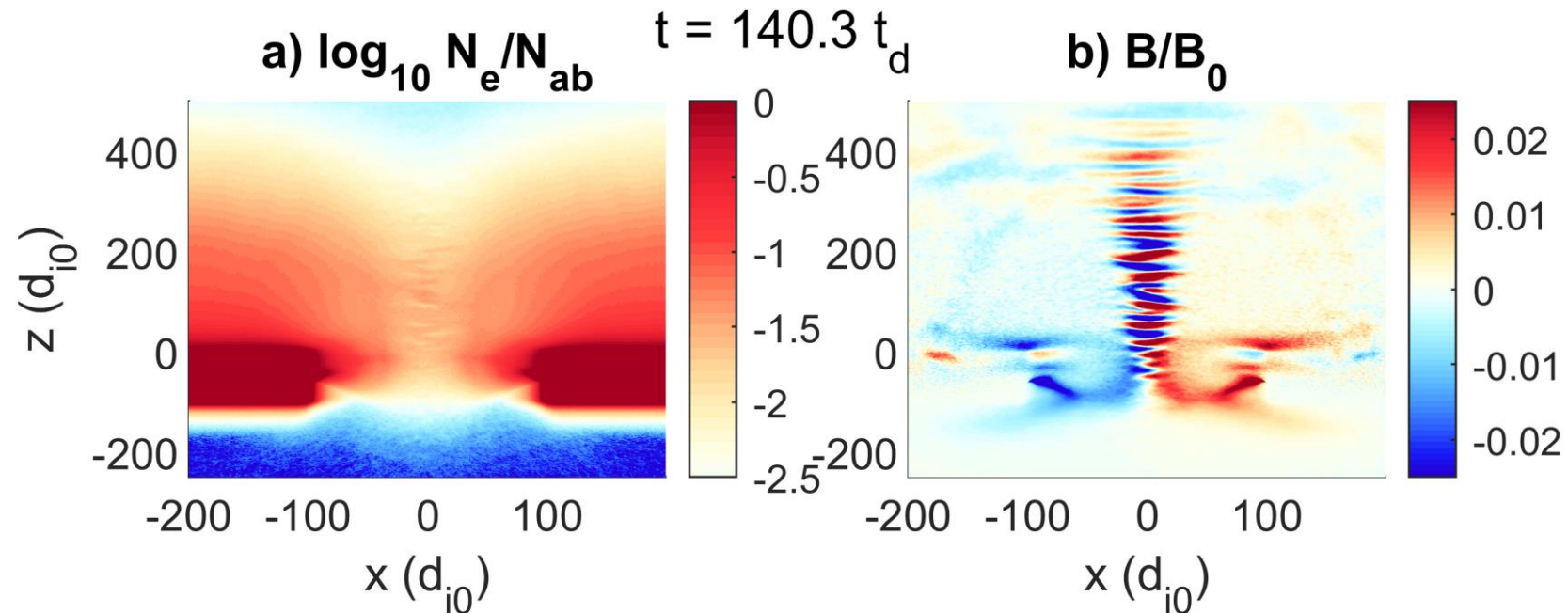
Evidence of Weibel in reconnection layer of Omega EP experiments

- EP refractometry indicates filamentation in the density
- PSC simulations show filamentation in density and field within the reconnection layer

Refractometry from Omega EP



Side-on PSC simulations of EP experiment



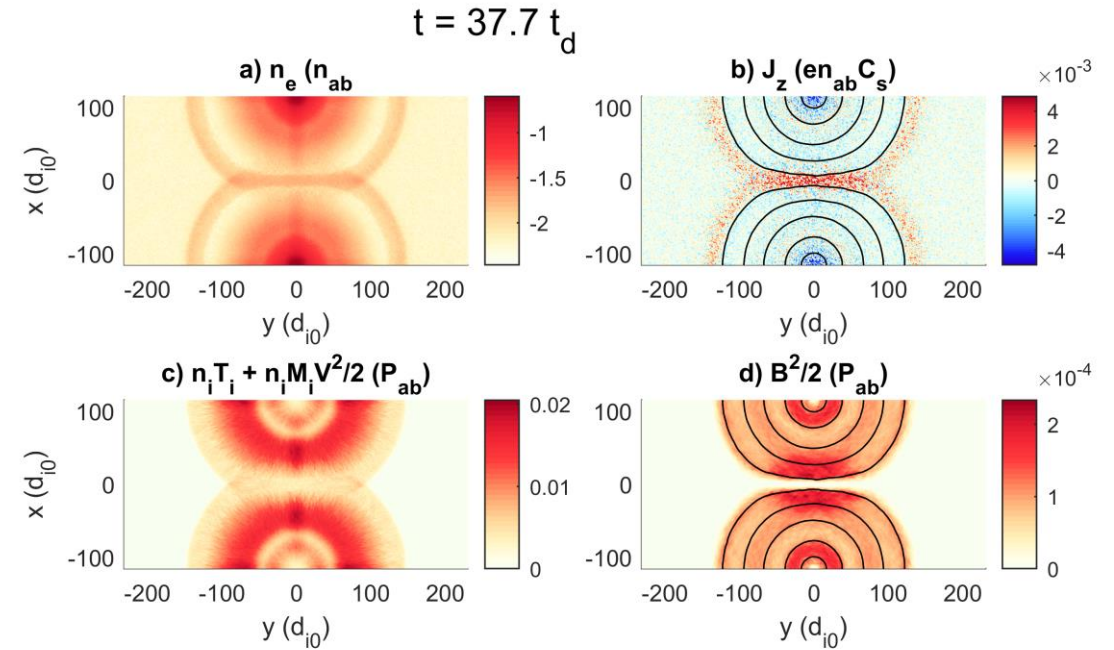
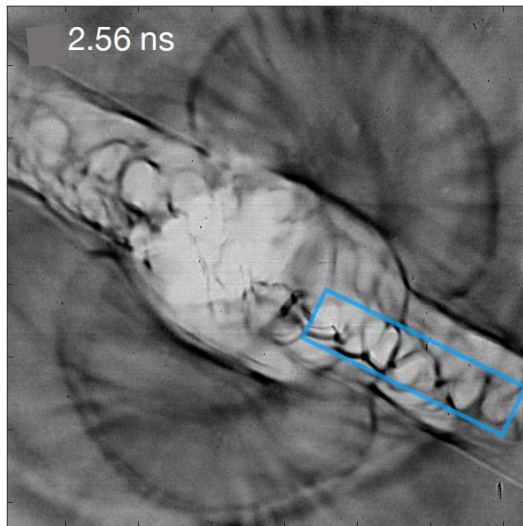
Can we recreate large number of plasmoid-like structures seen in Omega EP experiments?

Last year, we observed many plasmoid-like structures in Omega EP experiment via proton radiography.

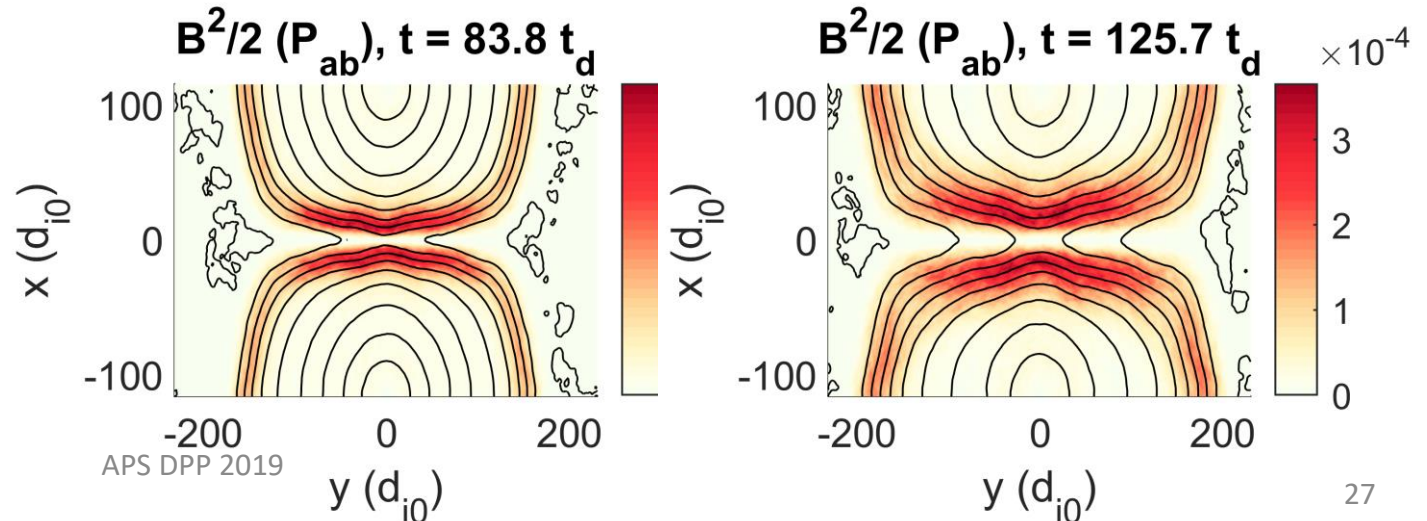
Taking a 1-D cut of ablations simulations, we can recreate Omega EP experiment; however no plasmoids observed.

We try many different 1-D cuts, where $B_{ram} \sim 100$, all show no plasmoids.

Proton Radiography data taken from recent EP campaign

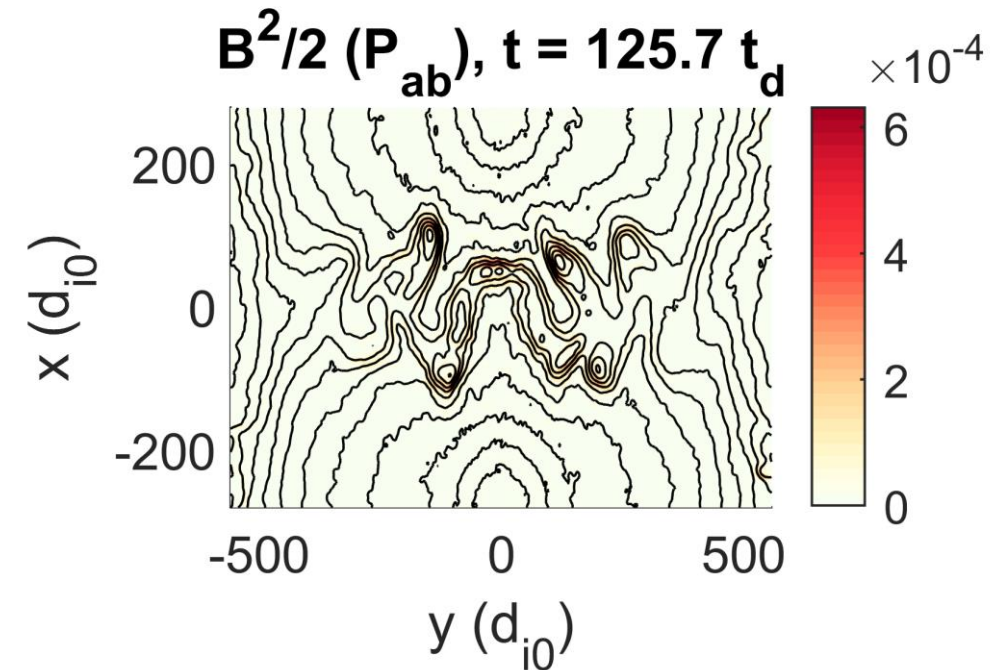
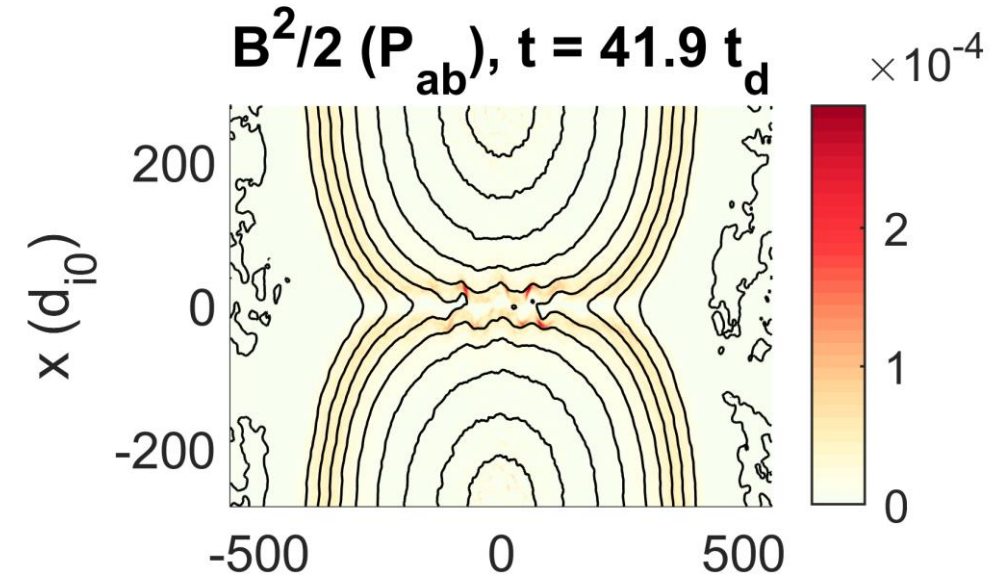
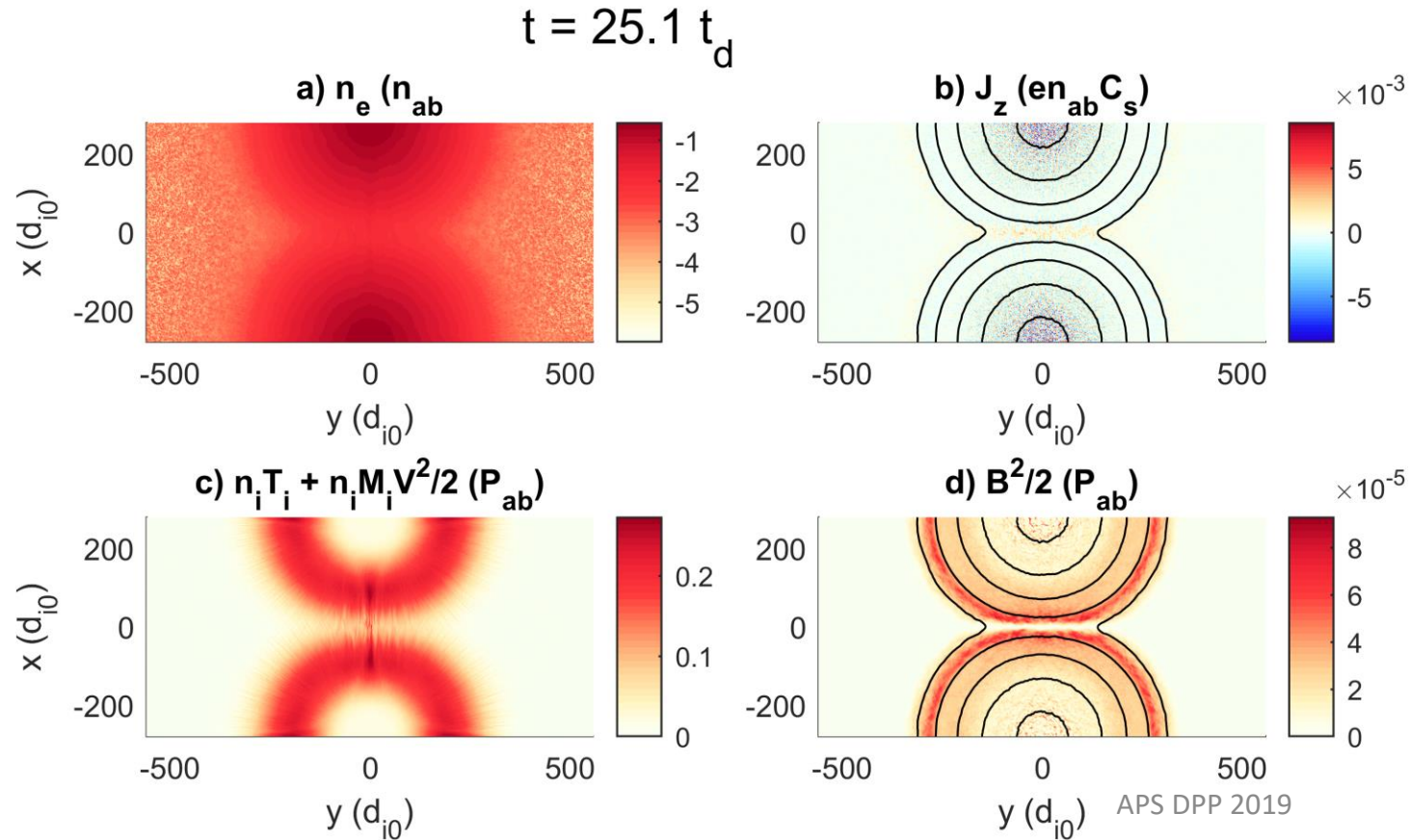


No plasmoids observed as reconnection simulations evolve



We observe plasmoids by increasing B_{ram} in the inflow

By increasing the inflow drive velocity, (now $B_{ram} \approx 2000$)
We find turbulent current sheet generated with large
number of plasmoid structures



Proton radiography qualitatively agrees with EP observations

Initial attempts proton radiography indicate similar caustic features directly corresponding to plasmoids

Results indicate that sufficient inflows (which will result in significant counter-streaming inside the reconnection layer) can result in a turbulent reconnection layer

2.8 ns

